01 Nov 1950

Four Papers on the Performance of Thin Walled Steel Structures

George Winter

Warner Lansing

R. B. McCalley Jr.

CORNELL UNIVERSITY

ENGINEERING EXPERIMENT STATION

REPRINT NO. 33

November 1, 1950

FOUR PAPERS ON THE PERFORMANCE OF THIN WALLED STEEL STRUCTURES

By George Winter,
Warner Lansing, and R. B. McCalley, Jr.

ENGINEERING EXPERIMENT STATION

REPRINT NO. 33

Stress Distribution in and Equivalent Width of Flanges of Wide, Thin-Wall Steel Beams, by George Winter. (Reprint from Technical Note No. 784, National Advisory Committee for Aeronautics, Washington, 1940.)

Performance of Thin Steel Compression Flanges, by George Winter. (Reprint from Preliminary Publication, Third Congress, International Association for Bridge and Structural Engineering, p. 137, Liege, 1948.)

Performance of Laterally Loaded Channel Beams, by George Winter, Warner Lansing, and R. B. McCalley, Jr. (Reprinted from Research, Engineering Structures Supplement [Colston Papers, vol. II], p. 49, London, 1949.)

Performance of Compression Plates as Parts of Structural Members, by George Winter. (Reprint from Research, Engineering Structures Supplement [Colston Papers, vol. II], p. 179, London, 1949.)

CORNELL UNIVERSITY
ITHACA, NEW YORK

Acknowledgment

THE INVESTIGATIONS reported in the four papers were carried out under the auspices of the Engineering Experiment Station of Cornell University, Dean S. C. Hollister, Director, and in the School of Civil Engineering, Professor W. L. Malcolm, deceased, and Professor N. A. Christensen, Directors.

They are part of, or related to, an extensive investigation of thin-walled steel structures sponsored jointly by the American Iron and Steel Institute and Cornell University, of which Professor George Winter, Head, Department of Structural Engineering, is in active charge. On the part of the Steel Institute the work is directed by the technical subcommittee of the Committee on Building Codes, Mr. Milton Male, Chairman, Mr. B. L. Wood, consulting engineer. The writers wish to acknowledge their sincere appreciation for the unfailing cooperation of these gentlemen.

NATIONAL ADVISORY COMMITTEE FOR AERONAUTICS

TECHNICAL NOTE NO. 784

STRESS DISTRIBUTION IN AND EQUIVALENT WIDTH OF FLANGES OF WIDE, THIN-WALL STEEL BEAMS*

By George Winter

SUMMARY

The use of different forms of wide-flange, thin-wall steel beams is becoming increasingly widespread. Part of the information necessary for a rational design of such members is the knowledge of the stress distribution in and the equivalent width of the flanges of such beams. This problem is analyzed in this paper on the basis of the theory of plane stress. As a result, tables and curves are given from which the equivalent width of any given beam can be read directly for use in practical design. An investigation is given of the limitations of this analysis due to the fact that extremely wide and thin flanges tend to curve out of their plane toward the neutral axis. A summary of test data confirms very satisfactorily the analytical results.

INTRODUCTION

This paper deals with the distribution of longitudinal stresses in the flanges of thin-wall beams of I-, T-, or box shape, or of similar shape.

Beams such as I- and other rolled sections and composites thereof have long been in use in structural engineering, and it is generally assumed that the magnitude of the longitudinal stresses does not vary over the width of the flange at a given cross section. With the development of light-weight construc-

---

*Condensed from a thesis accepted by the Graduate School of Cornell University in partial fulfillment for the degree of Doctor of Philosophy, June 1940.

This analysis was undertaken in parallel with an experimental investigation into this subject sponsored by the American Iron and Steel Institute at Cornell University.

with the web. It is then possible to investigate the resulting stress distribution by means of the theory of plane stress. The distribution of the shear stresses along the joint of web and flange evidently follows the distribution of the external shearing force in the beam as a whole. This assumption holds exactly only for beams loaded by continuously distributed loads. Concentrated loads result in local irregularities of the shear distribution because of the distributing action of the web and because of the actual area of application of such so-called concentrated loads. The influence of these factors will be investigated later in this paper. Thus the total shear T transmitted from the web to the flange at any particular cross section is proportional to the external shearing force V, namely,

$$T = \frac{m}{I} V = kV \tag{3}$$

where m is moment of area of flange about neutral axis and I is moment of inertia of the beam. The stress distribution of a plane plate loaded in that manner will now be analyzed.

Throughout this investigation the span of the beam is taken as 2ℓ and the width of the flange as 2b; the thickness of the flange is taken as unity. Thus figure 2(a) represents the flange of an I-beam loaded by a single concentrated force in the center; figure 2(b) shows the flange of a box beam under uniform load. Because the problem is one in plane stress, the solution reduces to the integration of the differential equation. (See reference 4.)

$$\frac{\partial^4 \varphi}{\partial x^4} + 2 \frac{\partial^4 \varphi}{\partial x^2 \partial y^2} + \frac{\partial^4 \varphi}{\partial y^4} = 0 \tag{4}$$

where φ is the Airy stress function. Then the stresses are

$$\sigma_x = \frac{\partial^2 \varphi}{\partial y^2} \tag{5a}$$

$$\sigma_y = \frac{\partial^2 \varphi}{\partial x^2} \tag{5b}$$

$$\tau_{xy} = - \frac{\partial^2 \varphi}{\partial x \partial y} \tag{5c}$$

where σ_x is the longitudinal stress; σ_y, the transverse stress; τ_{xy}, the horizontal shear stress. Equation (4) is satisfied by any function of the form

$$\varphi = \sum_{1}^{n} (A_n \cosh \alpha_n y + B_n \sinh \alpha_n y + C_n y \cosh \alpha_n y + D_n y \sinh \alpha_n y) \cos \alpha_n x \qquad (6)$$

where

$$\alpha_n = \frac{n\pi}{2l}$$

The constants A_n, B_n, C_n, D_n follow from the boundary conditions. By substitution of φ (equation (6)) in equation (5c) it is possible to represent the distribution of τ_{xy} along the loaded edge of the plate as a Fourier series. The boundary conditions common to both types of beams (see figs. 2(a) and 2(b)) are:

$$\sigma_y = 0 \text{ at } y = \pm b$$

and

$$\sigma_x = 0 \text{ at } x = \pm l$$

The second of these conditions is satisfied by making n odd. Two constants are required to satisfy the first condition. In addition, there are two more conditions in τ_{xy} along the longitudinal edges that vary according to the particular case. Thus, two more constants are required to satisfy these conditions, and hence all four constants are determined. It may be noted that this solution results in a set of horizontal shearing stresses along the short edges $x = \pm l$, which may or may not coincide with the actual distribution in any given beam, depending on the type of practical end support. However, because of equilibrium and symmetry, the resultant of these stresses is zero along either edge. Therefore, these stresses, according to Saint-Venant's principle, have only local effects, which disappear at a short distance from the edge. But from the designer's point of view only the stress distribution at and near the cross section of maximum moment, that is, near the center portion of the beam, is of interest. These stresses will not be affected by the shearing stresses along $x = \pm l$.

Having thus determined all four constants, one is able to compute the stresses at any point of the flange by means of equation (5) and the equivalent width from equation (2).

Stress Distribution in I- and T-Beams

The general solution just outlined applies only to plates loaded along their edges. Since, for I- and T- beams, the shear from the web acts along the center line of the flange, let the flange be cut in half along the x-axis. The distribution of these applied shear stresses at y = 0 is expanded in a Fourier series in sine only and with n odd. Let K_n be the coefficients of this series. Then the boundary conditions are:

(1) At $y = 0$, $\tau_{xy} = \sum_{1}^{n} K_n \sin \alpha_n x$

(2) At $y = b$, $\sigma_x = 0$

(3) At $y = b$, $\tau_{xy} = 0$

(4) Since the plate is cut in half along the x-axis, there is the further condition that the two halves are prevented from separating along the cut. Since bodily translation or rotation of either half is prevented by equilibrium and symmetry, this condition results at $y = 0$ in

$$\frac{\partial^2 v}{\partial x^2} = 0.$$

Conditions (1), (2), and (3) are evaluated by using for σ_x equation (5a), for τ_{xy} equation (5c), and for φ equation (6). In order to evaluate condition (4), let u be the displacement in the x-direction and v in the y-direction. Then the longitudinal strain

$$e_x = \frac{\partial u}{\partial x} = \frac{1}{E}(\sigma_x - \nu \sigma_y) = \frac{1}{E}\left(\frac{\partial^2 \varphi}{\partial y^2} - \nu \frac{\partial^2 \varphi}{\partial x^2}\right) \tag{7a}$$

and the shear strain

$$\gamma_{xy} = \frac{\partial u}{\partial y} + \frac{\partial v}{\partial x} = \frac{1}{G} \tau_{xy} = -\frac{1}{G} \frac{\partial^2 \varphi}{\partial x \partial y} \tag{7b}$$

where E is Young's modulus, ν is Poisson's ratio, and $G = \frac{E}{2(1+\nu)}$ is the modulus of elasticity in shear. If equation (7a) is differentiated with respect to y

$$\frac{\partial^2 u}{\partial x \partial y} = \frac{1}{E}\left(\frac{\partial^3 \varphi}{\partial y^3} - \nu \frac{\partial^3 \varphi}{\partial x^2 \partial y}\right) \tag{8a}$$

And if equation (7b) is differentiated with respect to x, with $\left(\frac{\partial^2 v}{\partial x^2}\right)_{y=0} = 0$

$$\left(\frac{\partial^2 u}{\partial x \partial y}\right)_{y=0} = -\frac{1}{G}\left(\frac{\partial^3 \varphi}{\partial x^2 \partial y}\right)_{y=0} \tag{8b}$$

If the right sides of equations (8a) and (8b) are equated, it is seen that at y = 0

$$-\frac{1}{G}\left(\frac{\partial^3 \varphi}{\partial x^2 \partial y}\right)_{y=0} = \frac{1}{E}\left(\frac{\partial^3 \varphi}{\partial y^3} - \nu \frac{\partial^3 \varphi}{\partial x^2 \partial y}\right)_{y=0} \tag{8c}$$

Equation (8c) and conditions (1), (2), (3), result in four simultaneous equations in A_n, B_n, C_n, D_n. Solving these, the four constants are

$$A_n = -K_n \frac{(1-\nu)\sinh^2 a_n b + (1+\nu)(a_n b)^2}{a_n^2(\sinh 2a_n b + 2a_n b)} \tag{9a}$$

$$B_n = K_n \frac{1-\nu}{2a_n^2} \tag{9b}$$

$$C_n = K_n \frac{1+\nu}{2a_n} \tag{9c}$$

$$D_n = -K_n \frac{(1+\nu)\cosh^2 a_n b + (1-\nu)}{a_n(\sinh 2a_n b + 2a_n b)} \tag{9d}$$

All these constants are expressed in K_n, that is, in terms of the Fourier coefficients of the shear distribution series along the loaded edges. It is therefore possible to adapt the solution to any given type of loading.

Stress Distribution in Box and U-Beams

The flanges of such beams are loaded by shearing stresses along both longitudinal edges. (See fig. 2(b)). The distribution of these stresses again is expanded in a Fourier series in sine only and with n odd, the coefficients of which are K_n. Then the boundary conditions are:

(1) At $y = \pm b$, $\tau_{xy} = \pm \sum_{1}^{n} K_n \sin \alpha_n x$

(2) At $y = \pm b$, $\sigma_y = 0$

(3) And by symmetry, at $y = 0$, $\tau_{xy} = 0$

If equations (5a), (5c), and (6) are used, four simultaneous equations are again arrived at from which

$$A_n = - K_n \frac{2b \sinh \alpha_n b}{\alpha_n(\sinh 2\alpha_n b + 2\alpha_n b)} \tag{10a}$$

$$B_n = 0 \tag{10b}$$

$$C_n = 0 \tag{10c}$$

$$D_n = K_n \frac{2 \cosh \alpha_n b}{\alpha_n(\sinh 2\alpha_n b + 2\alpha_n b)} \tag{10d}$$

Equivalent Width for Different Loading Conditions

In order to derive data for use in practical design, three kinds of loading are investigated for both types of beams and for different ratios of width to span, b/l. The types of loading and the corresponding shear distributions are shown in figure 3. These shear distributions are expanded in Fourier series in sine only and with n odd. The respective Fourier coefficients are:

For loading (a)

$$K_n = \pm \frac{1}{n^2} \tag{11a}$$

For loading (b),

$$K_n = \frac{1}{n} \tag{11b}$$

For loading (c),

$$K_n = \pm \frac{1}{n} \sin \frac{n\pi}{4} \tag{11c}$$

If these coefficients are introduced into equations (9) and (10), the stress function φ is then determined from equation (6).

In order to compute the equivalent width 2b', use is made of equation (2). Introducing into this equation σ_x from equation (5a)

$$2b' = \frac{2\int_0^b \sigma_x dy}{\sigma_{max}} = \frac{2\int_0^b \frac{\partial^2 \varphi}{\partial y^2} dy}{\sigma_{max}} = \frac{2\left.\frac{\partial \varphi}{\partial y}\right|_{y=0}^{y=b}}{\sigma_{max}} \tag{12}$$

The maximum stress σ_{max} (see fig. 1) occurs at the web, that is, at $y = 0$ in I-beams and at $y = \pm b$ in box beams. Thus,

$$\sigma_{max} = \left(\frac{\partial^2 \varphi}{\partial y^2}\right)_{y=0} \quad \text{for I beams, and}$$

$$\sigma_{max} = \left(\frac{\partial^2 \varphi}{\partial y^2}\right)_{y=b} \quad \text{for box beams}$$

For design purpose it is the ratio of the equivalent to the actual width 2b'/2b that is important. If σ_{max} is substituted into equation (12), one obtains for I-beams

$$\frac{2b'}{2b} = \frac{1}{b} \frac{\left.\frac{\partial \varphi}{\partial y}\right|_{y=0}^{y=b}}{\left(\frac{\partial^2 \varphi}{\partial y^2}\right)_{y=0}} \tag{13a}$$

and for box beams

$$\frac{2b'}{2b} = \frac{1}{b} \frac{\frac{\partial \varphi}{\partial y}\Big/_{y=b}}{\left(\frac{\partial^2 \varphi}{\partial y^2}\right)_{y=b}} \qquad (13b)$$

Having obtained the reduction factor 2b'/2b, it is then possible to determine the equivalent width of any given beam, multiplying the actual width by the appropriate reduction factor. The maximum stress is then obtained from the ordinary flexure formula

$$\sigma_{max} = \frac{M}{S'}$$

where M is the bending moment and S' is the reduced section modulus determined by using the equivalent width 2b' instead of the actual width 2b.

The stress concentration and hence the equivalent width vary along the beam. For concentrated loads the concentration is largest, that is, the equivalent width is the smallest, at the point where load is applied, which usually is also the section of maximum moment. For beams with uniformly distributed load, the maximum moment acts at the center of the span, and hence it is this place for which the reduction factor is to be determined. For use in design, reduction factors pertaining to the sections just mentioned have been computed for a wide range of span: width. It is easily seen that the reduction factors for loading (b) and (c) of figure 3 are identical. A comparison of equations (11b) and (11c) reveals that K_n for loading (c) is obtained from K_n for loading (b) through multiplication by $\overset{+-}{_{-+}} \frac{1}{\sqrt{2}}$. For loading (b), however, the critical cross section is the center of the span where $\cos \alpha_n x = \cos 0 = 1$; whereas for loading (c) it is the quarter points where $\cos \alpha_n x = \cos \frac{n\pi}{4} = \overset{+-}{_{-+}} \frac{1}{\sqrt{2}}$.

Hence, the stresses at that point are obtained from those at the center for loading (b) by multiplying the series for σ_x, term by term, by 1/2. Since this factor appears both in the numerator and in the denominator of the reduction factor 2b'/2b (see equation (12)), the equivalent widths for both types of concentrated loads are identical.

It is therefore safe to apply this reduction factor to any type of concentrated loading.

In table I numerical data are given for the reduction factors of both types of beams investigated and for distributed and concentrated loading.

TABLE I

Ratios of Equivalent to Actual Width, $2b'/2b$

Beams	I- and T-		Box and U-	
l/b	$p^{(a)}$	$p^{(b)}$	$p^{(a)}$	$p^{(b)}$
π	0.857	0.575	0.880	0.557
2π	.958	.791	.957	.778
3π	.981	.881	.983	.881
4π	.990	.927	.989	.926
5π	.993	.949	.994	.950

$^{(a)}p$ is uniformly distributed load

$^{(b)}P$ is concentrated load at center of span or two equal concentrated loads at quarter points.

The only numerical results given in Schnadel's paper on box beams (reference 2) pertain to a beam of ratio span: width = π. For this beam Schnadel found for $2b'/2b$ the following values: 0.553 for center load, 0.882 for uniformly distributed load, and 0.547 for quarter-point loads. It is seen that the differences between the results obtained by Schnadel's cumbersome method and those obtained by present simple approach are negligible for all practical purposes.

It follows from table I that the reduction factors for I- and T- beams are practically identical with those for box and U-beams except for extremely wide beams. For design work the values for I- and T-beams may therefore be used also

for box and U-beams. For more convenient use these factors are presented in figure 4 in the form of two curves from which for any particular beam and loading the reduction factor can be read immediately.

EXPERIMENTAL VERIFICATION

In order to facilitate an experimental test of these analytical results, it seems desirable to develop data that can be directly measured on test specimens. For this reason the ratios $\sigma_{max}/\sigma_{min}$ have been computed for I-beams, where

$$\sigma_{max} = \left(\frac{\partial^2 \varphi}{\partial y^2}\right)_{y=0} \quad \text{and} \quad \sigma_{min} = \left(\frac{\partial^2 \varphi}{\partial y^2}\right)_{y=b}$$

The results are given in table II.

TABLE II

Ratios of Maximum Stress at Web to Minimum Stress at Edge of Flange for I-beams, $\sigma_{max}/\sigma_{min}$

ℓ/b	p	P
π	1.30	2.50
2π	1.07	1.46
3π	1.03	1.23
4π	1.015	1.14
5π	1.005	1.09

Extensive experimental work has been carried out to check the analytical results. It included wide-flange rolled sections (d = 0.27 inch) and cold-formed beams made of thin sheets (d = 0.077 inch and d = 0.049 inch). A range of ℓ/b from 4 to 18 has been covered and center loading as well as

quarter-point loading has been investigated. Strains were measured by means of Huggenberger strain gages and stresses were computed from the strains. Because this test work is part of an extensive research program, sponsored by the American Iron and Steel Institute, the experimental details will be reported elsewhere. The results are summarized in figure 5, which gives the theoretical curves and the experimental results for the eleven beams tested. It is seen that the coincidence of empirical and analytical results is very close throughout the entire range. For this reason it is believed that the equivalent widths computed analytically may safely be recommended for use in design.

EFFECT OF DISTORTION OF CROSS SECTION

The foregoing analysis is based on the assumption that the flange may be regarded as a plane plate, thus allowing the application of the theory of plane stress. All other authors dealing with this problem have made the same assumption without investigating its validity for wide beams of thin sheet material. Actually, however, the flange is not only curved longitudinally in the loaded beam, but, under the action of the longitudinal bending stresses, also tends to curve in the direction perpendicular to the axis of the beam. For this reason it is necessary to investigate whether or not this double curvature materially affects the stress distribution.

An exact solution of this question would require a mathematical apparatus inappropriately involved for the given purpose. For this reason an approximate method will be used sufficiently exact for the present purpose.

Figure 6(a) represents a part of an I-beam in pure bending; figure 6(b) gives a short element ab of the bottom flange. It is seen that, because of the curvature of the loaded beam, the tensile forces H per unit width of the flange act at an angle $d\varphi$ and hence have a resultant R bisecting this angle, that is, acting in a radial direction. Because H is distributed over the entire width of the flange, R is similarly distributed. Therefore this resultant R acts as a force perpendicular to the surface of the flange tending to bend the flange inward toward the neutral axis. For this reason the distance from the flange surface to the neutral axis becomes smaller at the outer

than at the inner portions of the flange. Because the bending stresses are proportional to this distance to a degree of accuracy sufficient for the present purpose, they decrease from the web toward the edges.

From figure 6(b) it is seen that, per unit length of flange,

$$R = H \frac{d\varphi}{ds} = \frac{H}{r} = \frac{\sigma_x d}{r} \tag{14}$$

where r is the radius of curvature of the bent beam. As shown in figure 6(c), this R represents a transverse load tending to bend the flange. The differential equation for the bending of a long rectangular plate (from reference 5, equation (67)) is:

$$\frac{d^2w}{dy^2} = -\frac{1}{r} = -\frac{M}{D} \tag{15}$$

where w is the deflection of flange

D the flexural rigidity of plate $\left(\frac{Ed^3}{12(1 - \nu^2)}\right)$ and d the thickness of plate

It is seen that equation (15) is of the same type as the differential equation for the bending of beams

$$\frac{d^2w}{dy^2} = -\frac{M}{EI}$$

except that the beam rigidity EI is replaced by the plate rigidity D. For an exact solution the differential equation

$$d^4w/dy^4 = p/D$$

for cylindrical shells should be used, where p is the total transverse force and consists of R and of the elastic reaction. It can be shown that for the present purpose the numerical difference between the results based upon this exact approach and those obtained by using equation (15)

are negligible. Hence the familiar formulas for the deflections of beams can be applied to those of the flange if EI is replaced by D. On this basis the maximum deflection w_{max} (see fig. 6(c)) of the flange out of its plane will now be determined.

It is assumed that σ_x and thereby R can be taken as constant throughout the width of the flange which is sufficiently exact for small values of w. Then for I-beams from the ordinary cantilever formula (see reference 6, p. 356)

$$w_{max} = \frac{Rb^4}{8D} \tag{16}$$

For an investigation of the stress distribution under actual working conditions, let σ_w be the working stress. Then the radius of curvature r of the beam is determined from

$$r = \frac{EI}{M} \quad \text{with} \quad M = \frac{2\sigma_w I}{h}$$

to

$$r = \frac{Eh}{2\sigma_w} \tag{17}$$

where I is the moment of inertia of the beam. If equation (17) is substituted in equation (14)

$$R = 2\sigma_w^2 \frac{d}{Eh}$$

And from equation (16)

$$w_{max} = 2\sigma_w^2 \frac{b^4 d}{8DEh} = 3\left(\frac{\sigma_w}{E}\right)^2 \frac{b^4}{d^2 h}(1 - \nu^2) \tag{18}$$

The value of w_{max} having been determined, it follows from the linear variation of σ_x over the depth of the cross section that the ratio of the maximum stress at y = 0 to the minimum stress at $y = \pm b$ is

$$\frac{\sigma_{max}}{\sigma_{min}} = \frac{h}{h - 2w_{max}} \tag{19}$$

If the same considerations are applied to box and U-beams and if the generally weak restraint of the flange at the web is neglected, the flange may be regarded in this case as a simple plate freely supported at the webs. From reference 6, p. 350,

$$w_{max} = \frac{5}{384} \frac{RL^4}{D} \tag{20a}$$

or, since here the span L = 2b,

$$w_{max} = \frac{5}{24} \frac{Rb^4}{D} \tag{20b}$$

and using again equations (15), (16), (17)

$$w_{max} = 5\left(\frac{\sigma_w}{L}\right)^2 \frac{b^4}{d^2 h} (1 - \nu^2) \tag{21}$$

If this w_{max} is introduced in equation (19), the stress decrease due to the distortion of the cross section can again be determined.

It is thus seen that the curvature of the beam results in itself in a nonuniform stress distribution in the flanges, which is an effect entirely different from that investigated before on the basis of the distribution of the shearing forces. An exact investigation should therefore consider the joint action of both those effects. It can be shown, however, that in beams of practically possible dimensions the effect of the curvature of the beam is exceedingly small and may therefore be neglected in practical applications.

In order to establish a criterion indicating in which case the effect of the curvature of the beam may be neglected, it will be assumed that a stress decrease of 4 percent is negligible for all practical purposes. Such a stress decrease results in a reduction of the equivalent width of less than 2 percent, which is less than any attainable design accuracy. It is therefore necessary to establish a criterion such that

$$\sigma_{max} - \sigma_{min} \leqq 0.04\ \sigma_{max} \tag{22}$$

Because the stresses are proportional to the distances from the neutral axis, if equation (18) is used for I-beams

$$\frac{w_{max}}{h/2} = 6\left(\frac{\sigma_w}{E}\right)^2\left(\frac{b^2}{dh}\right)^2(1 - \nu^2) \leqq 0.04$$

or

$$\frac{b^2}{dh} \leqq \frac{0.0817\ E}{\sqrt{1 - \nu^2}\,\sigma_w} \tag{23a}$$

and, in particular, for steel beams with $E = 3 \times 10^7$ pounds per square inch

$$\frac{b^2}{dh} \leqq \frac{2.57 \times 10^6}{\sigma_w} \tag{23b}$$

where b, h, d are, respectively, half the flange width, the depth, and the flange thickness of the beam; σ_w, the working stress; and ν, Poisson's ratio.

Similarly for box beams, if equation (21) is used

$$\frac{w_{max}}{h/2} = 10\left(\frac{\sigma_w}{E}\right)^2\left(\frac{b^2}{dh}\right)^2(1 - \nu^2) \leqq 0.04$$

or

$$\frac{b^2}{dh} \leqq \frac{0.0633\ E}{\sqrt{1 - \nu^2}\,\sigma_w} \tag{24a}$$

and particularly for steel beams

$$\frac{b^2}{dh} \leqq \frac{1.98 \times 10^6}{\sigma_w} \tag{24b}$$

employing the same symbols as above.

Hence, the data for the equivalent width given in table I and figure 4 may be applied to any beam satisfying the conditions expressed in equations (23) and (24). It may

easily be verified numerically that practically all beams with structurally possible dimensions will satisfy these conditions.

CONVERGENCE OF THE SERIES INVOLVED

In the foregoing analysis, the reduction factor $2b'/2b$ as well as the stress concentration $\sigma_{max}/\sigma_{min}$ are obtained as quotients, the numerator and the denominator of which are in the form of a Fourier series. The numerical values given in tables I and II have been obtained by taking nine terms of each of the series involved. In order to obtain an estimate of the accuracy thus obtained, it seems advisable to analyze the question of the convergence of these series. This analysis will be made here for I-beams only because the method is essentially the same for box beams.

In order to investigate the numerator of equation (13a), the coefficients A_n, B_n, C_n, D_n from equations (9) are substituted in equation (6), which results in

$$\left.\frac{\partial \varphi}{\partial y}\right|_{y=0}^{y=b} = \sum_{1}^{n} \frac{K_n}{\alpha_n}$$

Substitution of the appropriate K_n from equations (11) gives for uniformly distributed load

$$\sum_{1}^{n} \frac{K_n}{\alpha_n} = \sum_{1}^{n} \pm \frac{1}{n^2} \frac{2\ell}{n\pi} = \sum_{1}^{n} \pm \frac{\text{const}}{n^3}$$

and for concentrated load

$$\sum_{1}^{n} \frac{K_n}{\alpha_n} = \sum_{1}^{n} \frac{1}{n} \frac{2\ell}{n\pi} = \sum_{1}^{n} \frac{\text{const}}{n^2}$$

It is seen that each of these expressions is an absolutely convergent series, the first few terms of which decrease rather rapidly.

Making the same substitutions in the denominator of equation (13a), one arrives at

$$\left(\frac{\partial^2\varphi}{\partial y^2}\right)_{y=0} = \sum_1^n (A_n\alpha_n^2 + 2D_n\alpha_n)$$

$$= -\sum_1^n K_n \frac{(3+\nu)\cosh^2\alpha_n b + (1-\nu) + (1+\nu)(\alpha_n b_n)^2}{2\sinh\alpha_n b\cosh\alpha_n b + 2\alpha_n b}$$

Because the hyperbolic functions involved increase exponentially with α_n, it is seen that for higher terms (α_n large) the individual terms of this series approach the corresponding terms of

$$\sum_1^n K_n \frac{3+\nu}{2}\coth\alpha_n b \cong \frac{3+\nu}{2}\sum_1^n K_n$$

because for large α_n $\coth\alpha_n b \cong 1$. If for uniformly distributed load K_n is substituted from equation (11a), it is seen that the higher terms of this series are of the type $\sum_1^n \pm\frac{\text{const}}{n^2}$, which again is absolutely convergent. For concentrated load, however, substitution of K_n from equation (11b) gives a series the higher terms of which are seen to approach those of the series $\sum_1^n \frac{\text{const}}{n}$ while the first few terms of the former series decrease more rapidly than those of the latter. Hence, the series for the denominator of equation (13a) for concentrated load is divergent, although the individual terms approach zero with increasing n and the first few terms decrease rather rapidly.

In a purely mathematical sense this divergence does not threaten the validity of the solution. Indeed, φ (equation (6)) satisfies the original differential equation (4) not only as a series but term by term. Hence, the series may be broken off at any arbitrary term and the sum will still satisfy equation (4) and all other equations derived from it. Therefore, the problem consists in the physical rather than in the mathematical legitimacy of taking a small number of terms of a divergent series.

It will be remembered that by means of the first of the four boundary conditions the given shear distribution

at y = 0 is expressed in a Fourier series, the coefficients of which are K_n. In order to obtain full coincidence of this series with the shear diagram of figure 3(b), one would have to take an infinite number of terms. Breaking the series off after nine terms means that the discontinuous curve of figure 3(b) is replaced by a continuous, though sharply changing, curve. As an example such a curve, but for four terms, is given in figure 7(a) (reference 7, p. 63). For nine terms, part a of this curve will be correspondingly shorter. If one now regards the closely corresponding curve of figure 7(b) as the diagram of shear distribution it is seen that it corresponds to a loading of the kind of figure 7(c) rather than to an ideally concentrated load. The length a is equal to one-half the wave length of the last sine wave added, i.e., to span/n or in our case to span/17. However, the actual shear distribution will just be of this same kind for the following two reasons: All concentrated loads actually are distributed over a small length c (fig. 7(c)) of the span and, before reaching the flange, the resulting shear will be further distributed in the web. Therefore, by taking a definite number of terms, the analysis is based on a shear distribution which, in essence, is exactly of the kind actually occurring under concentrated loads.

It remains to verify whether taking nine terms of the corresponding series is sufficiently accurate for the given purpose. This question may be answered in the affirmative for the following three reasons:

1) In actual structures concentrated loads usually are distributed over a length along the span of not less than span/50. Without detailed investigation of this question, it may safely be assumed that the further distribution in the web doubles or even triples this length.

2) The reduction factor $2b'/2b$ changes very little with decreasing values of a. For instance, for a beam of $\ell/b = 2\pi$, $2b'/2b = 0.828$ for six terms and $2b'/2b = 0.791$ for nine terms. Thus an increase in the length a of about 55 percent (span/11 instead of span/17) results in an increase of less than 5 percent in the equivalent width. For higher terms this difference becomes still smaller.

3) The experimental results summarized in figure 5 have been obtained by applying loads in some cases directly through rollers and, in other cases, through distributing plates of width = span/24 to span/48. The good coincidence of analytical and empirical results is sufficient proof for the adequacy of the chosen number of terms.

GENERAL CONCLUSION

The primary purpose of the investigation was to analyze the stress distribution in the flanges of wide, thin-wall beams of I, T-, U-, and box shape and to obtain results suitable for direct application in design. It is shown that the magnitude of the bending stresses in the flanges of such beams varies across the width of the section and that the amount of this variation depends upon the dimensions of the beam and upon the type of loading.

Therefore, in the determination of the magnitude of the maximum bending stress in design work, the equivalent width of such flanges should be used instead of the actual width. In figure 4 curves are given from which this equivalent width can be read directly for any particular type of beam and loading.

For the purpose of facilitating the experimental verification of the analytical results, further curves have been computed that give the ratios of the maximum to the minimum bending stress in the flanges. These ratios have been checked experimentally by means of strain measurements on 11 I-beams. The experimental data confirm very satisfactorily the analytical results.

It is further shown that the cross sections of wide beams made of extremely thin sheets are subject to distortion that gives rise to additional stress concentration. Equations (23) and (24) furnish simple conditions for determining the limiting dimensions of beams for which the effect of this distortion may be neglected in practical applications. It may easily be verified numerically that practically all beams of structurally possible dimensions will satisfy these conditions.

College of Engineering, School of Civil Engineering,
Cornell University, Ithaca, N. Y., June 1940.

REFERENCES

1. von Kármán, Th.: Die mittragende Breite (The Effective Width), pp. 114-127 of Beiträge zur technischen Mechanik und technischen Physik (Contributions to Technical Mechanics and Technical Physics). (Festschrift, August Föppl). Julius Springer (Berlin) 1924.

2. Schnadel, G.: Die mittragende Breite in Kastenträgern und im Doppelboden. Werft Reederei Hafen, no. 5, March 7, 1928, pp. 92-101.

3. Chwalla, E.: Formulas for the Determination of Effective Width of Thin Flange and Rib Plates. Der Stahlbau, vol. 9, no. 17, May 8, 1936, pp. 73-78.

4. Timoshenko, S.: Theory of Elasticity. McGraw-Hall Book Co., Inc., 1st ed., 1934, p. 25.

5. Timoshenko, S.: Strength of Materials. Vol. II. D. Van Nostrand Co., Inc., 1930, p. 476.

6. Anon.: Steel Construction; a Manual for Architects, Engineers and Fabricators of Buildings and Other Steel Structures. Amer. Inst. of Steel Const., 1939.

7. Byerly, W. E.: An Elementary Treatise on Fourier's Series and Spherical, Cylindrical, and Ellipsoidal Harmonics, with Applications to Problems in Mathematical Physics. Ginn and Co., 1893, p. 63.

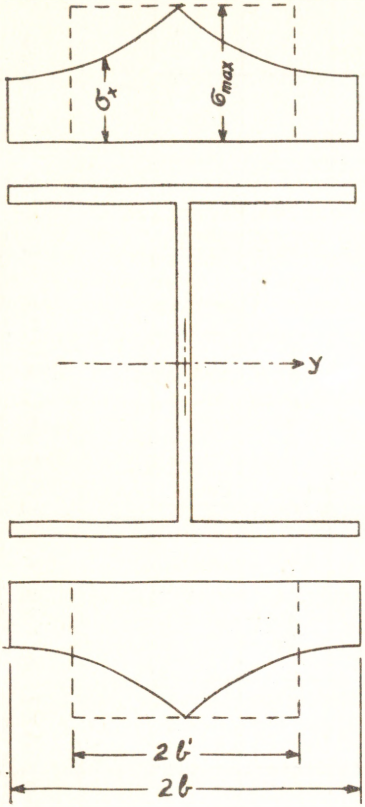

Figure 1.- Actual stress distribution over width of flange of I-beam.

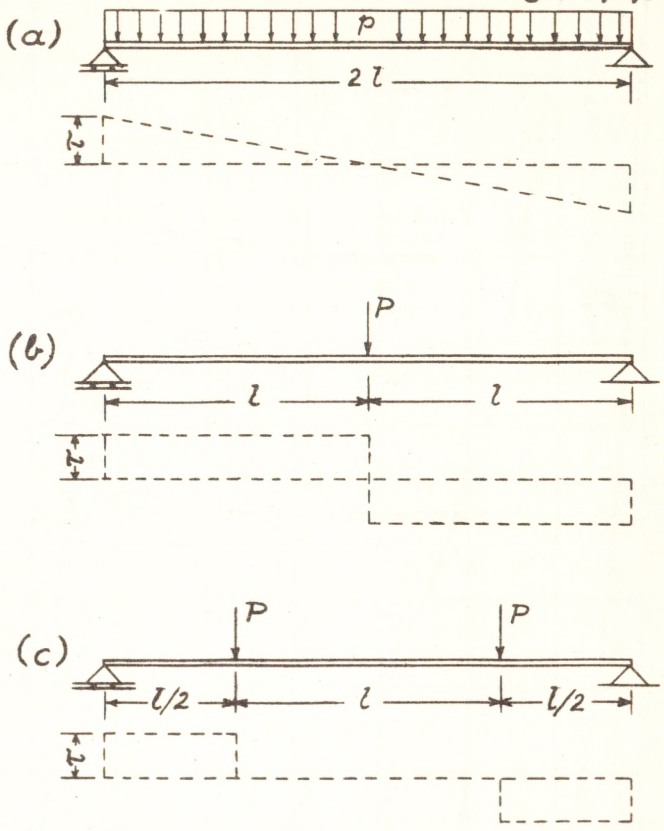

Figure 3.- Shear distribution for the three types of loading analyzed. (a) Uniformly distributed load. (b) Single concentrated load applied in the center. (c) Two concentrated loads of equal magnitude applied at quarter points.

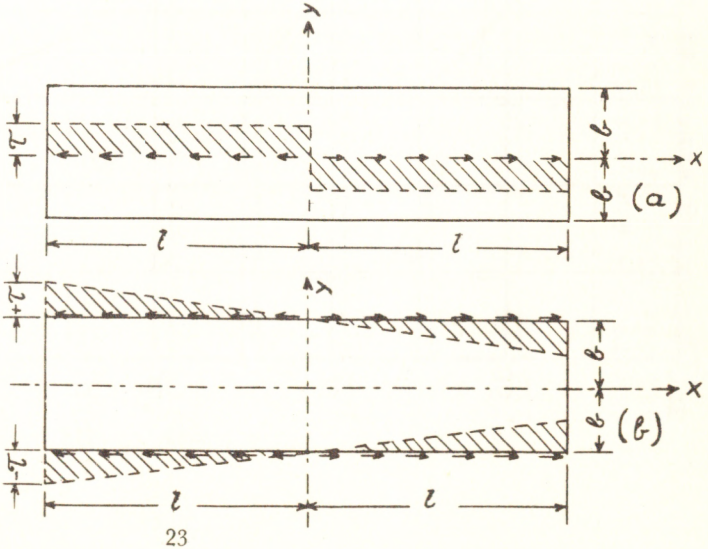

Figure 2.- Distribution of applied shear stress, transmitted from web to flange. (a) Flange of I-beam loaded by a single concentrated force in the center. (b) Flange of box beam under uniform load.

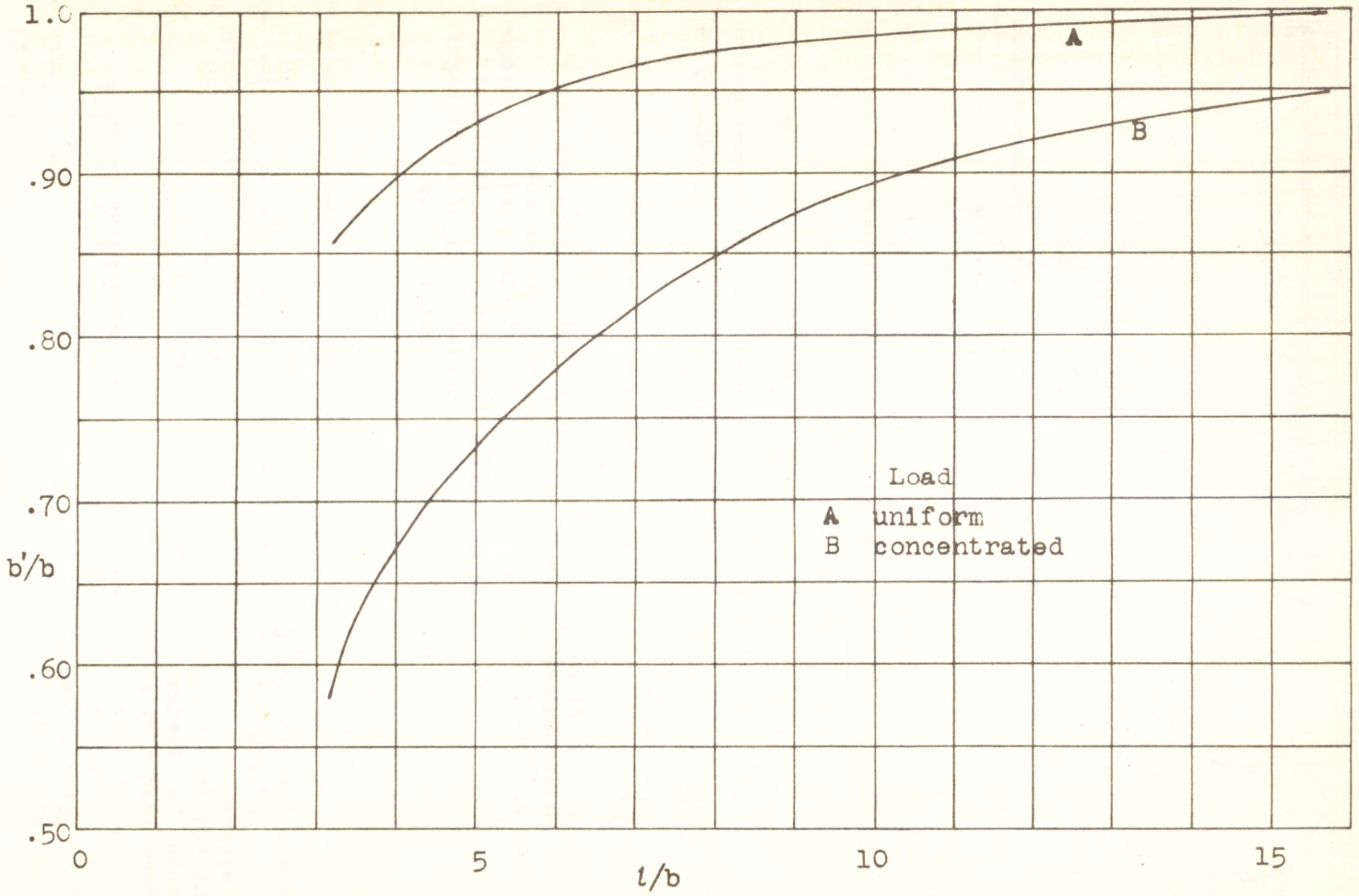

Figure 4.- Analytical curves for determining the equivalent width of the flanges of I-, T-, U-, and box beams. l/b = span/width, b'/b = equivalent width/actual width.

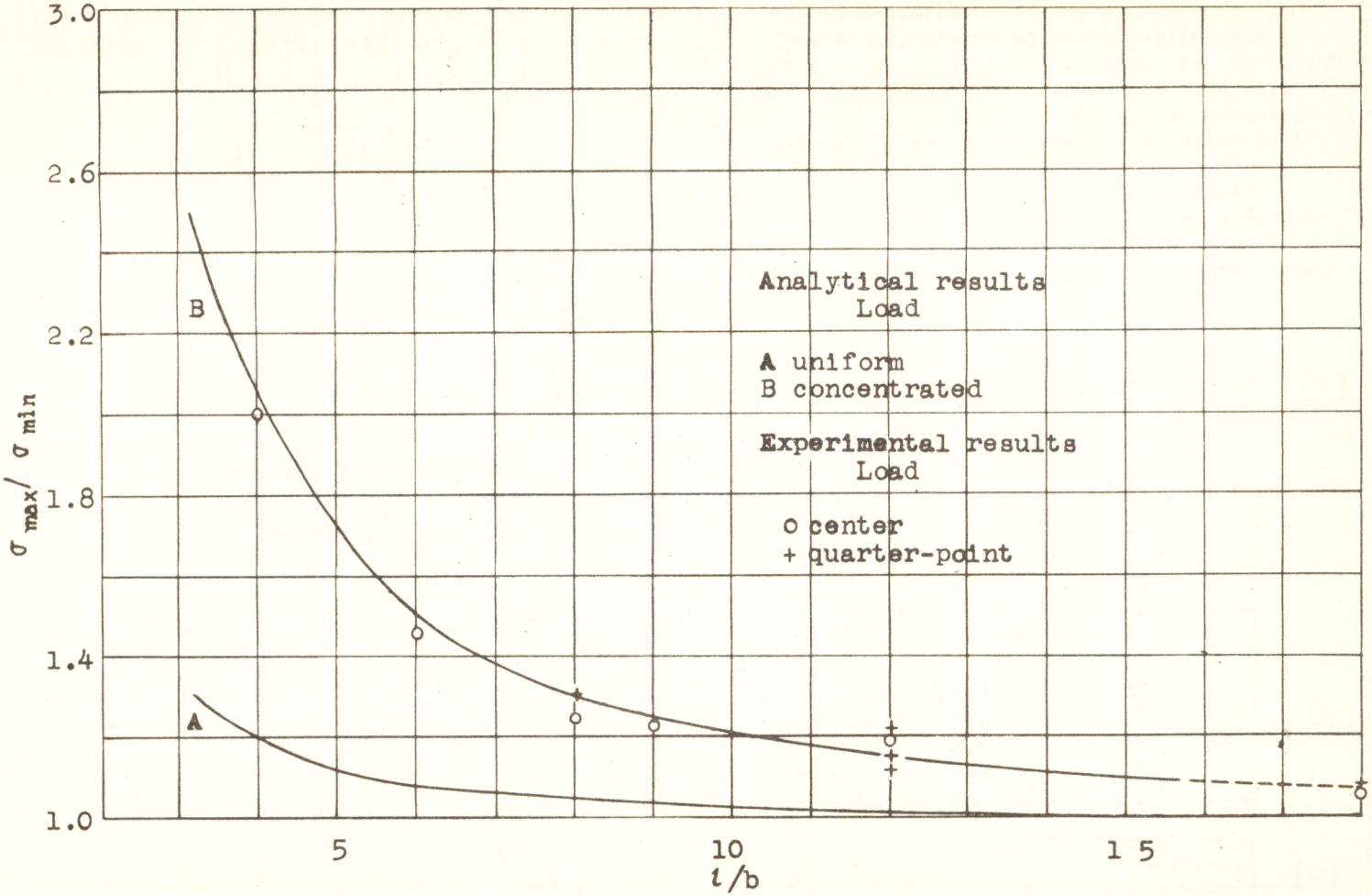

Figure 5.- Analytical stress concentration curves for I- and T-beams and experimental resualts of 11 I-beams tested. σ_{max}=bending stress at joint of web and flange, σ_{min}=bending stress at outer edge of flange, l/b span/width

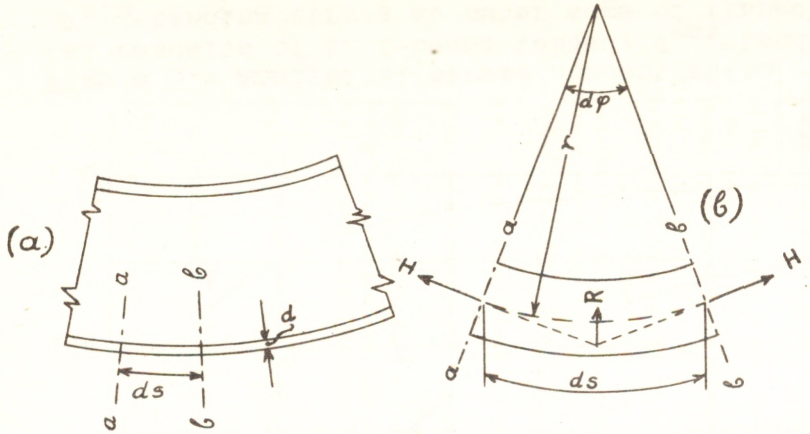

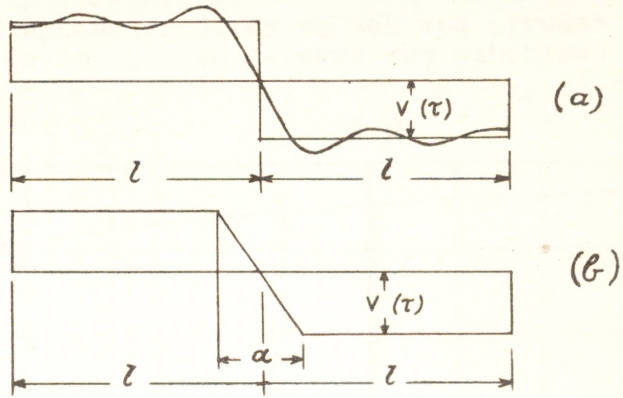

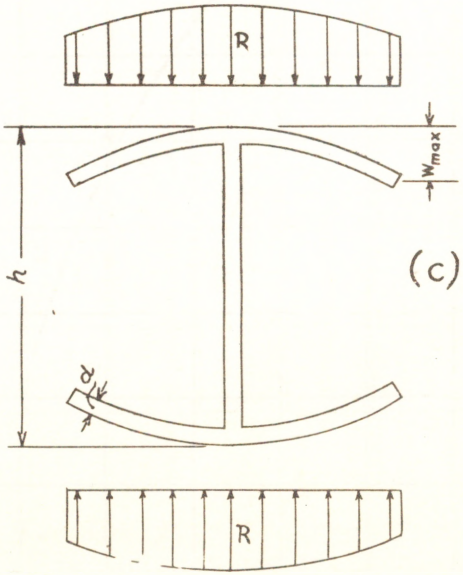

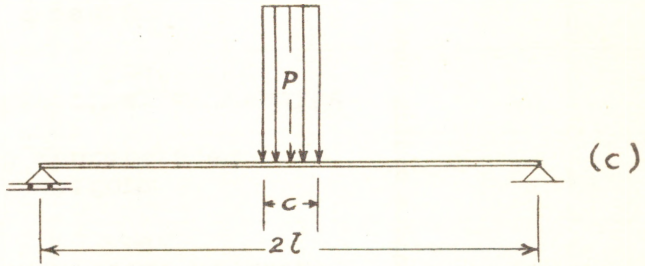

Figure 7.- Shear distribution of beam loaded by concentrated force in center; representation of the actual shear distribution by four terms of a Fourier series.

Figure 6.- Actual stress distribution over width of flange due to distortion of cross section of I-beam. (a) Side-view of section of I-beam. (b) Element, ab, of bottom flange. (c) Distorted cross section and stress distribution.

Performance of thin steel compression flanges

D[r] GEORGE WINTER
Professor of Structural Engineering, Cornell University, Ithaca, N. Y., U. S. A.

The economic use of standard, hot-rolled steel shapes is limited to relatively substantial structures. The need for lighter steel members for small scale industrial, commercial and residence building initiated the use of structural members made from sheet steels by cold forming (cold rolling or pressing). Roof decks of a considerable variety of sizes and shapes, formed in this manner, as well as structural shapes of I-, channel, and similar sections, have been in use in the U. S. A. for many years. The development of automatic spot welding on the one hand, and the wartime demand for light, pre-fabricated buildings on the other, have stimulated this development.

It was soon realized, however, that accepted design procedures had to be modified to suit the special requirements of such thin-walled structures. The American Iron and Steel Institute, in 1939, inaugurated a research program under the writer's direction at Cornell University, which has resulted in the « Specifications for the Design of Light Gage Steel Structural Members » issued by the Institute in 1946.

One of the main problems in this connection is that of the performance of thin compression plates, both at loads causing failure and at the lower design loads. In this connection two types of such plates must be distinguished :

a) Long plates that are stiffened along both longitudinal edges, such as webs of channels and I-beams;

b) Long plates that are stiffened only along one longitudinal edge, such as the flanges of channels, I-sections, and angles.

The present paper is concerned only with the first of these two types.

The classical theory of elasticity allows the calculation of critical buckling loads of such plates by the so-called small deflection theory, that is by the solution of the differential equation

$$\frac{\partial^4 w}{\partial x^4} + 2\frac{\partial^4 w}{\partial x^2 \partial y^2} + \frac{\partial^4 w}{\partial y^4} = -\frac{st}{D}\frac{\partial^2 w}{\partial x^2} . \qquad (1)$$

In contrast to the phenomenon of column buckling, the critical stresses calculated from eq. 1 do not represent the limit of carrying capacity of edge supported plates. Indeed, in such plates, deflections can not increase indefinitely, as they do in columns at the Euler load. Consequently, once the critical stress is passed, the hitherto plane plate merely deforms into a non-developable, wavy surface, but continues to resist increasing stress. The deformations just described result in additional, particularly transverse stresses which act jointly with the imposed, primary longitudinal compression stress. In analyzing this state one can no longer neglect the influence of the deflections on the distribution of stress, which had been the basis for the development of eq. 1.

The differential equation for this large deflection buckling of plates was developed by Th. v. Kármán in 1910, and reads as follows

$$\frac{\partial^4 w}{\partial x^4} + 2\frac{\partial^4 w}{\partial x^2 \partial y^2} + \frac{\partial^4 w}{\partial y^4} = \frac{t}{D}\left(\frac{\partial^2 F}{\partial y^2}\frac{\partial^2 w}{\partial x^2} - 2\frac{\partial^2 F}{\partial x\,\partial y}\frac{\partial^2 w}{\partial x\,\partial y} + \frac{\partial^2 F}{\partial x^2}\frac{\partial^2 w}{\partial y^2}\right) \qquad (2)$$

where F is a stress function. The complexity of this equation has so far prevented its explicit solution for rectangular plates. It is for this reason that this problem had to be investigated primarily by experimental methods.

In this connection the concept of the equivalent width, initiated by Th. v. Kármán, proved most helpful. This concept is best visualized by means of a model. Imagine a square compressed plate replaced by a lattice of bars. Beyond the buckling load of the compressed rods the lattice will obviously distort in the manner shown in fig. 1. Two circumstances are clear from this picture :

a) The compression bars cannot fail as simple columns by continued deflection because they are restrained from doing so by the cross-bars.

b) In the stage shown in the figure the total load is obviously not equally distributed among the compression bars; in view of the variations of the deflections the bars near or at the edges carry more load than those near

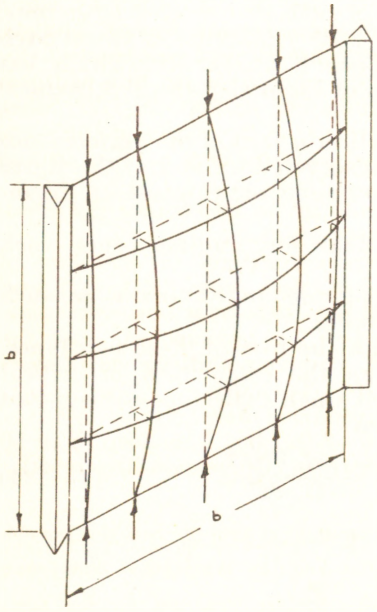

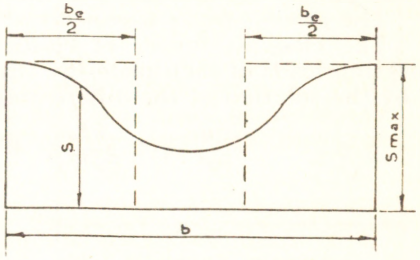

Fig. 1 (left) and Fig. 2 (right).

the center, and failure will occur when the more heavily loaded bars will reach their yield strength.

It can be seen, therefore, that after first buckling has occurred, the stress in a compressed plate must show a distribution as given in fig. 2. The effective width b_e is that width which will make the area under the dotted lines equal to the area under the actual solid stress curve. Once this effective width is determined, design can proceed in the usual manner, merely by replacing the actual plate area $b \times t$ by the equivalent area $b_e \times t$. T. v. Kármán gave the following tentative expression for this effective width at the failure load :

$$b_e = \frac{\pi}{\sqrt{3(1-\nu^2)}}\, t \sqrt{\frac{E}{s_{yp}}} = 1{\cdot}9\, t \sqrt{\frac{E}{s_{yp}}} \qquad (3)$$

for Poisson's ratio $\nu = 0.3$ (1).

Subsequent tests by E. E. Sechler showed that this expression was reasonably correct for very wide and thin plates, but that a smaller value of b_e results for plates of smaller b/t-values (2).

All these investigations were concerned only with the determination of the ultimate or yield strength of such plates. In addition, the amount of test evidence even in this respect was limited.

For practical design, however, it is necessary to determine equivalent widths not only at failure, but also at smaller loads, in particular at service loads. Indeed, since slight buckling occurs for large b/t at loads far below the ultimate, the stress distribution of the type of fig. 2 takes place not only at failure but frequently at design loads. Hence, in a flexual member of the type of fig. 3, stresses and corresponding deformations are distributed at design loads in the manner shown. The neutral axis of such a member is then located below the centroid of the area, and its location as well as the moment of inertia, section modulus, etc. must be computed by using the equivalent instead of the real width of the compression flange. That is, in order to compute stresses, deflections, and other design information for any load up to failure, the actual section, fig. 3*a*, with its non-uniform stress distribution can be replaced by the equivalent section, fig. 3*b*. Since the maximum stresses, and corresponding strains, at the edges of the webs are equal for these two sections, all required information can be gained from this equivalent section.

It was therefore necessary for practical design to determine the effective width not only at failure, but also at lower loads.

For this purpose more than 100 tests were carried out on members of the type of fig. 3, and other shapes, with b/t-ratios from 14 to 429 and with steel yield points from 20 100 to 57 800 psi. Deformations were measured in these flexural tests and it was found, as anticipated, that the neutral axis was located below the centroid, and was shifting downward under increasing load, i.e. with decreasing effective width.

Only the most recent of these tests are reported here (3).

Specimens of these tests were of the type of fig. 3*a*, 3 in deep, 5 to 10 in wide, with thicknesses from 0.0288 tot 0.0615 in. Corresponding width/

---

(1) Th. v. Kármán, E. E. Sechler, L. H. Donnell, *The Strength of Thin Plates in Compression* (*Trans. Am. Soc. Mech. Eng.*, Vol. 54, 1932, p. 53).

(2) E. E. Sechler, *The Ultimate Strength of Thin Flat Sheet in Compression*, Publication No. 27, Guggenheim Aeronautics Labor, Pasadena, Cal., 1933.

(3) Geo. Winter, *The Strength of Thin Steel Compression Flanges* (*Proc. Am. Soc. Civ. Eng.*

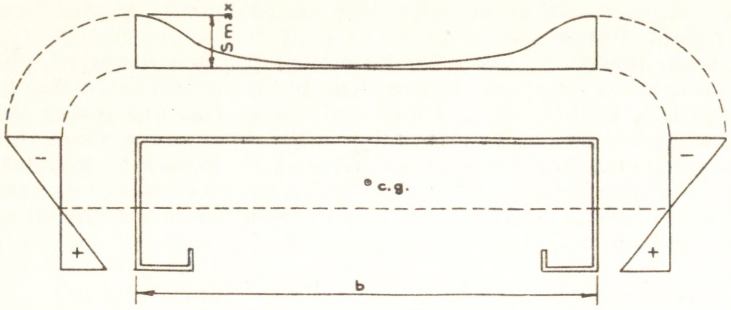

Fig. 3a.

thickness ratios b/t ranged from 86 to 344, yield points of steels, from tension tests, were found to range from 24 400 to 56 850 psi. Specimens were tested as beams, with two equal loads at the quarter points of the span. In addition to deflections, strains were measured at the top and bottom of the flanges, allowing an experimental determination of the position of the neutral axis. Finally, displacements of the top flange out of its original plane were measured at six points along the center line, in the portions of the beams between loads.

Information on the magnitude of the equivalent width was gained from these tests in the following manner : The position of the neutral axis, at various loads, was established from strain gage readings. Knowing this position, in a section like fig. 3*b*, it is simple to compute the corresponding value of b_e. With the equivalent section determined in this manner, the maximum compression stress s_{max} corresponding to the particular load is computed by customary methods. The tests, therefore, give information on the relation of b_e to b/t and s_{max}.

To evaluate this relation, eq. 3 is rewritten as

$$b_e = Ct\sqrt{\frac{E}{s_{max}}} \tag{4}$$

where C is a coefficient to be determined from test. Previous investigations by Sechler and the writer ([2]) ([3]) established that C depends primarily on the non-dimensional parameter $\sqrt{\frac{E}{s_{max}}}\left(\frac{t}{b}\right)$. It is for this reason that, in fig. 4, the experimentally determined coefficients C are plotted against this parameter. Determinations were made, for each test specimen, at the yield load and at 1/3 and 2/3 of that load.

Although the scattering of test results, as depicted in fig. 4, is quite considerable it is clearly seen that the coefficient C decreases with increasing $\sqrt{\frac{E}{s_{max}}}\left(\frac{t}{b}\right)$ The scattering is apparently due to the extreme sensitivity of this method to very minor experimental deviations. Indeed, a variation of 1 % in the experimentally determined location of the neutral axis will cause, in many cases, a variation of 10 % and more of the value of C. For

Vol. 72 p. 199, 1946 and *Trans. Am. Soc. Civ. Eng.*, Vol. 112, p. 1, 1947). See also *Bull.* No. 35, Part 3, Cornell University Engg. Experiment Station, Ithaca, N. Y., 1947.

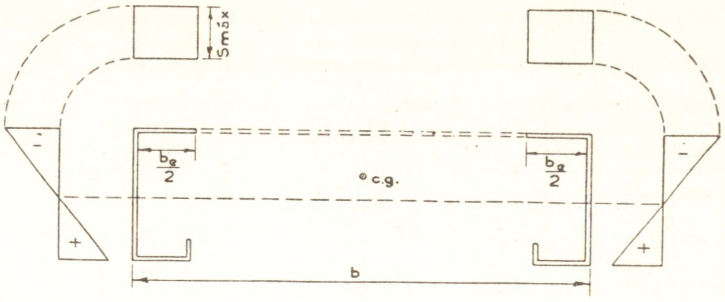

Fig. 3b.

this reason, in interpreting fig. 4, the data should be regarded as statistically distributed, rather than as strictly accurate.

With this in mind, the straight line drawn on that figure was thought to represent a reasonable, and somewhat conservative means of developing a simple formula for the equivalent width b_e. The line is seen to start at a value of 1.9 for extremely large b/t-values and relatively high stresses, for which case, therefore, the experimental determinations are in substantial agreement with v. Kármán's original eq. 3. The formula for b_e obtained from this straight line can be written as

$$b_e = 1.9\, t \sqrt{\frac{E}{s_{max}}} \left(1 - 0.475 \frac{t}{b} \sqrt{\frac{E}{s_{max}}}\right) \qquad (5)$$

which is seen to be identical with eq. 3, except for the modifying term in parenthesis, which, as pointed out, approaches 1 closely for large b/t and s_{max}.

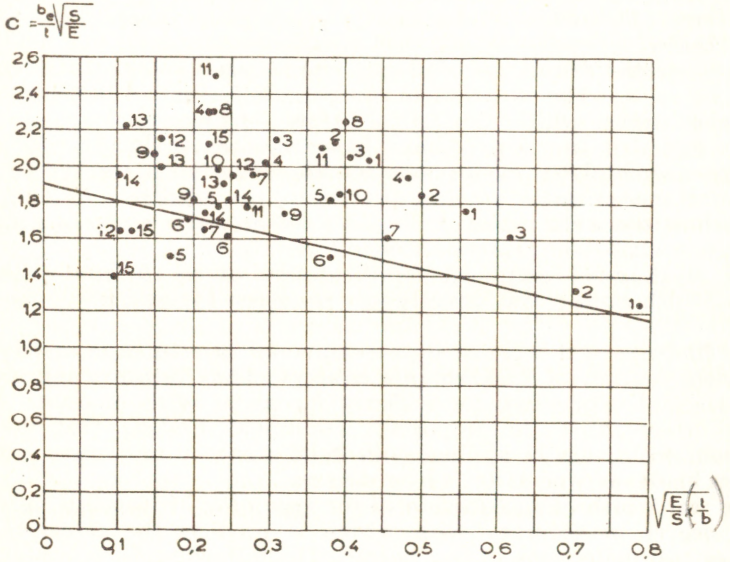

Fig. 4.

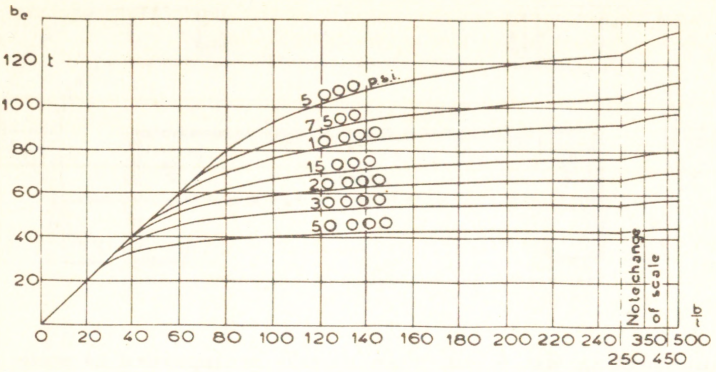

Fig. 5. Effective width of compression elements stiffened along both edges.

Eq. 5 indicates that a compression plate is fully effective (uniform stress distribution, $b_e = b$) for values of b/t smaller than

$$\left(\frac{b}{t}\right)_L = 0.95\sqrt{\frac{E}{s_{max}}} \qquad (6)$$

and that, for values above $(b/t)_L$ deformations, deflections, and yield loads can be calculated with good accuracy by using the effective instead of the real width.

By solving eq. 6, for s_{max}, it can easily be calculated that the first redistribution of stress, that is the first gradual formation of buckling waves occurs at stresses equal to $s_{cr}/4$, where s_{cr} is the critical buckling stress obtained from the small deflection theory, i.e. from eq. 1. This result is not amazing. Theoretically, an ideally plane plate should not buckle at stresses below s_{cr}. Actual sheet steel members, however, are not perfect but possess initial distortions of shape, which result in small deflections at stresses below s_{cr}. The situation is comparable to that of initially bent or eccentric columns, which also deflect below the Euler load.

The fact that the initial shape has a definite influence on the performance of such plates, causes considerable scattering of test results. These are also influenced by the amount of restraint provided by adjoining members, such as the webs in fig. 3. For this reason eq. 5 represents merely a conservative statistical expression of test results.

Fig. 5 shows a graphical representation of eq. 5 from which the effective width can be read directly for any given b/t and E/s_{max} for use in design.

The findings of this primarily experimental investigation merely represent an elaboration of v. Kármán's concept. They improve the accuracy of his original expression, particularly for plates with moderate b/t. In addition, they prove the important additional finding that the same expression, eq. 5, can be applied with good accuracy to stresses occurring at design loads, as well as to failure stresses.

The real worth of an equation of the type of eq. 5 depends, of course, on the degree of accuracy with which it predicts the actual carrying capacities and deflections of test beams. The following table contains, for the 15 beams whose results are plotted on fig. 4, the yield loads as deter-

mined from test, and those computed by means of the equivalent section, fig. 3*b*, using eq. 5 for determining the equivalent width.

N°	b/t	Yield Point psi	Yield Load, Computed lb	Yield Load Test lb	Deviation %
1	95	27 500	2 660	2 300	— 13.5
2	86	36 000	3 640	3 600	— 1.1
3	109	37 400	2 730	2 500	— 8.4
4	145	30 150	1 480	1 550	+ 4.7
5	175	25 750	964	1 100	+ 14.1
6	172	24 700	945	1 025	+ 8.5
7	155	25 850	1 160	1 200	+ 3.4
8	175	47 200	4 520	4 500	— 0.4
9	163	56 850	5 570	5 500	— 1.3
10	222	24 400	1 845	1 760	— 4.6
11	216	36 050	2 550	2 250	— 11.8
12	284	30 650	1 523	1 480	— 2.8
13	303	25 100	1 165	1 280	+ 9.9
14	339	28 000	1 052	940	— 10.7
15	344	27 650	1 028	1 060	+ 3.0
					average deviation — 0.7 %

It is seen that, for a very wide range of b/t and yield point stress, eq. 5 allows the prediction of the actual carrying capacity with very satisfactory accuracy. The same was found to be true for the numerous earlier tests ([3]).

It is interesting to note that despite the rather bad scattering of some points on fig. 4, such as points 4, 8, 11 and 15, the predicted and actual carrying capacities of these four beams, as given in the table, are in very satisfactory agreement. This supports the opinion advanced before that the scattering in fig. 4 is due mainly to inevitable inaccuracies in the empirical determination of the neutral axes.

For practical design, deflections are of interest at design loads rather than at yield loads. Since b_e depends on the value of s_{max}, the effective moment of inertia is variable and must be determined for any given load. The « Design Specifications » mentioned in the introductory paragraphs stipulate a factor of safety of 1.85. For this reason, a comparison of measured and computed deflections is given in the table below for loads approximately equal to the computed yield loads divided by 1.85. Further computations, the results of which are omitted here, show that the same general picture as given in this table obtains for other values of loads, up to the yield load. The table gives the deflections d measured in tests at the load P, and the deflections computed for that load (a) by using the equivalent width b_e and (b) by using the full unreduced width b.

N°	P lb	d, from test in	d, computed using b_e, in	%	d, computed using b in	%
1	1 465	0.090	0.091	— 1.1	0.085	+ 5.6
2	2 000	0.120	0.118	+ 1.7	0.111	+ 8.1
3	1 495	0.128	0.131	— 2.3	0.108	+ 18.5
4	811	0.108	0.097	+ 10.2	0.076	+ 42.1
5	526	0.076	0.072	+ 5.6	0.055	+ 38.2
6	514	0.068	0.068	0.0	0.054	+ 25.9
7	635	0.078	0.075	+ 4.0	0.060	+ 30.0
8	2 500	0.128	0.161	— 20.5	0.122	+ 4.9
9	3 080	0.170	0.195	— 12.8	0.148	+ 14.9
10	1 010	0.072	0.083	— 13.3	0.064	+ 12.5
11	1 395	0.102	0.119	— 14.2	0.089	+ 14.6
12	833	0.083	0.100	— 17.0	0.066	+ 25.8
13	635	0.061	0.074	— 17.6	0 055	+ 10.9
14	574	0.075	0.078	— 3.9	0.052	+ 44.2
15	559	0.077	0.075	+ 2.7	0.050	+ 54.0
				Average deviation — 5.2 %		Average deviation + 23.3 %

The table shows that by using the effective width b_e deflections are computed with an average accuracy of about 5 %, whereas the use of the full, unreduced section for this purpose leads to an average error of about 23 %. Though scattering is again considerable, all significant discrepancies in the first case are on the safe side (computed deflections larger than measured values). On the other hand, by using the full, unreduced sectional area, errors on the unsafe side in several cases reach magnitudes of 40-50 %; by this method, for all beams, actual deflections were found to be larger than computed.

It should be said that an accurate computation of deflections by the equivalent width method would involve the use of a moment of inertia, variable along the beam. Indeed, since b_e depends on s_{max}, the effective moment of inertia increases from a minimum value at the point of maximum moment to a maximum value near the supports. In the table above, however, only the minimum moment of inertia was used. For the present tests this does not lead to too large an error, since M_{max} is constant over the center half of the span, for quarter point loading. Had a variable moment of inertia been used, all deflections computed by using b_e would have been obtained slightly smaller, to various relative degrees, resulting in a still better average agreement with test results. This method of calculation was not used because, in routine design procedures, engineers can hardly be expected to spend the very considerable amount of time necessary for such detailed calculations with variable moment of inertia.

The evidence presented above, which is additionally supported by a great number of other tests previously published elsewhere ([3]) indicates that the proposed method allows, with reasonable accuracy, the determination of carrying capacities as well as deflections of members containing thin compression flanges. The measure of agreement with test results is not as close as would be obtained on customary, heavy steel structures. This, however, is predicated on the inherent character of thin sheet material with its inevitably larger imperfections as to accuracy of sheet

thickness, of geometrical shape, etc. The discrepancies obtained in these tests are believed to be tolerable practically; they are certainly not larger than these observed in tests of reinforced concrete or timber structural members.

The use of eq. 5 is somewhat cumbersome for routine design computations. The graph of fig. 5 allows the direct determination of b_e for any given stress and b/t-ratio. The initial straight line to which all curves are tangent indicates the range over which the full width b is effective. It is seen that the larger the maximum stress, the smaller is that limiting b/t beyond which the effectiveness of the flange begins to decrease (see eq. 6).

In contrast to conventional, thick-walled steel structures, the cross-sections of thin-walled elements distort at loads far below the ultimate, and in most cases at values even below the design loads. The type and magnitude of these deformations is therefore of interest, since an excessive amount of flange distortion would obviously make such members practically objectionable even if their strengths and over-all deflections were adequate for the purpose.

These distortions of shape, for members of the type of fig. 3, consist of two separate kinds of deformation which superpose to result in the final shape under load. The first, and more obvious, is the simple buckling deformation. Indeed, ultimate stresses and frequently working stresses are considerably above the critical buckling stress as determined from eq. 1. Moreover, it was mentioned in connection with eq. 6 that on the basis of this equation incipient, extremely slight flange distortions apparently occur at stresses of the order of $s_{cr}/4$. Consequently, at stresses of about that magnitude, the compression flange begins to buckle into a series of approximately quadratice buckling waves. That is, the half-wave length is about equal to the flange width b, and the general shape of each of these half-waves is that schematically indicated on fig. 1. This type of deformation, which was observed in all tests of this kind, is of course exactly the one predicted by the mathematical theory of buckling of plates.

In beam specimens of the type discussed herein, however, a fundamentally different type of deformation is superposed on the one just discussed. This type, which was likewise observed in all tests, is not limited to compression flanges; it occurs likewise if the beams of fig. 3 are turned by 180° so that the wide flange is in tension. The following brief and intentionally approximate analysis illustrates the nature of these deformations and allows a reasonably accurate determination of their magnitude.

Consider an element of the flange, of unit width in the transverse direction, and length dl longitudinally, as shown on fig. 6. Under load, this element is curved, its radius, r_b, being equal to that of the beam at that cross-section. The total compression forces at both ends of the element consequently subtend an angle $d\varphi$ and, therefore have a resultant

$$R = st\,\frac{d\varphi}{dl} = \frac{st}{r_b}\,. \tag{7}$$

If the stress s is uniform over the width of the cross-section, R acts in the same manner as an external, transverse load, as shown in fig. 6*a*, tending to bend the flange toward the neutral axis. This bending is governed by the simple equation for flexure of a long, narrow rectangular plate under transverse load, i.e.

$$\frac{d^2y}{dx^2} = -\frac{1}{r_c} = -\frac{M_f}{D}\,. \tag{8}$$

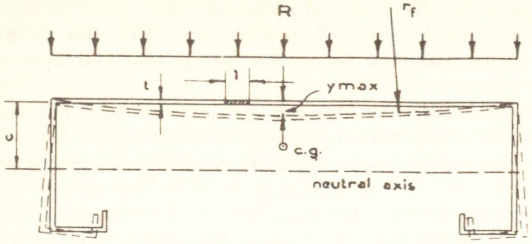

Fig. 6a.

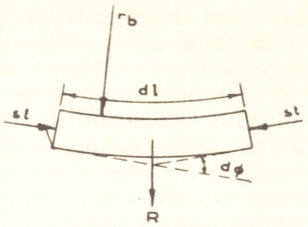

Fig. 6b.

The maximum deflection is then found from the usual formula

$$y_{max} = \frac{5}{384} \frac{st}{r_b} \frac{b^4}{D} . \tag{9}$$

The use of this formula neglects the influence of restraint provided to the flange by the webs. However, this restraint is of rather undetermined magnitude. The webs of isolated beams deform as shown on fig. 6*a*, and therefore afford little restraint. The restraint would be larger if such beams were laid side by side, with webs in contact, as in a floor. In view of this indeterminacy it seems best to neglect the unreliable effect of possible restraint.

To find r_b for substitution in eq. (9) one has from standard, elementary beam theory

$$r_b = \frac{EI}{M_b} ; \quad M_b = \frac{sI}{c} ; \quad r_o = \frac{Ec}{s} . \tag{10}$$

With this value of r_b, the maximum flange distortion becomes

$$y_{max} = \frac{5}{32} \left(\frac{s}{E}\right)^2 \frac{b^4}{t^2 c} (1 - \nu^2) . \tag{11}$$

For tension flanges with their generally rather uniform stress distribution, this type of distortion is the only one that occurs and its magnitude can be determined with satisfactory accuracy from eq. 11. In compression flanges the longitudinal stresses vary over the width of the flange as shown on fig. 2. Consequently, R is likewise distributed in this manner, instead of the uniform distribution shown on fig. 6*a*. In view of the approximate character of this calculation, and of the uncertainty as to the amount of edge restraint, the details of the actual distribution of *s*, and other factors, an elaborate modification of eq. 11 to account for the stress distribution of fig. 2 would represent a rather fictitious improvement. For this reason it is believed that a sufficiently close approximation is obtained, if, in eq. 11, the average stress of fig. 2 is substituted for *s*. From the definition of the equivalent width, this average stress is easily obtained from

$$s_{av} = s_{max} \left(\frac{b_e}{b}\right) . \tag{12}$$

For more information on this type of deformation, particularly for tension flanges, see the writer's earlier paper (4).

---

(4) Geo. Winter, *Stress-Distribution in, and Equivalent Width of Wide, Thin-Wall Steel Beams*, Techn. Note No. 784. Advisory Comm. for Aeronautics, 1940, Washington, D. C.

In the tests reported herein, both types of deformation were clearly observed. That is, the flanges showed a general « dishing » (smooth downward deflection of the center line) on which was superposed the square-wave pattern of the buckling deformations. By means of special apparatus, the magnitude of these distortions of the flanges perpendicular to their original planes were measured at six points along the center line of each beam. It was found that at design loads (i.e. about $P_{yield}/1.85$) these deformations reached a maximum of 1 % of the flange width for two of the beams; and in most other cases they were closer to 1/2 %. Although these distortions are clearly visible, it can be said that their magnitude at design loads is sufficiently small so as not to interfere with the practical use of such light gage steel members.

In conclusion it should be said that the information given in this paper suffers from the evident disadvantage of being primarily empirical and approximate. The theoretical complexity of plate buckling at stresses larger than s_{cr}, as well as the large amount of possible variations of shape resulting in a wide range of conditions of edge restraint, precluded an analytical treatment of practical value. It is hoped that future investigations in this field, both mathematical and experimental, will elucidate some of the more detailed aspects of this problem.

NOTATION

b = flat width of flange.
b_e = equivalent flange width.
c = distance from neutral axis to extreme fiber.
D = flexural plate rigidity.
$= E\ t^3/12\ (1-\nu^2)$.
M_b = bending moment in beam.
M_f = bending moment in flange.
r_b = radius of curvature of beam.
r_f = radius of curvature of flange.
s = stress in flange.
s_{cr} = critical buckling stress of flange by small deflection theory.
s_{yp} = yield stress of material.
t = flange thickness.
w = buckling deflection of flange.
x, y = coordinates.
ν = Poisson's ratio.

Performance of Laterally Loaded Channel Beams

G. WINTER, W. LANSING and R. B. McCALLEY

Channel shapes are rarely used as beams loaded in the plane of the web in view of their tendency to twist. In steel construction of the usual type shapes which do not possess this tendency are manufactured at no extra cost. In light gauge steel construction members are produced by cold forming of sheet steel, and the channel is the most economically manufactured two flange shape. This paper, on the basis of theoretical and experimental evidence, presents methods of determining the spacing and strength of bracing required to counteract the twisting tendency of such members. A general theory of elastic behaviour of such members is briefly indicated; it allows determination of stresses and rotations of channels loaded by forces in the plane of the web. Experimental evidence on these latter quantities is presented together with test information on the ultimate carrying capacity as it is affected by location of braces. From the latter data it is concluded that localized maximum stress does not govern the strength of such members since plastic stress redistribution allows the initially understressed portions of the section to carry additional load. If this action is taken into account it is shown that maximum efficiency can be obtained with a reasonably small number of braces in the span.

THE use of channels as transversely loaded beams is severely restricted by the fact that their shear centre is not coincident with the centroid, which results in twist of the member unless it is loaded in a plane through the shear centre and parallel (or perpendicular) to the web. For this reason channel sections ordinarily are not used in this manner since doubly symmetrical I-sections, which do not manifest this disadvantage, are just as easily manufactured by the hot rolling process as are channel shapes.

The situation is different, however, in the rapidly expanding field of light gauge steel construction, for which structural shapes are manufactured from sheet steel by cold forming, either by means of press-brakes or by cold rolling. Channel sections are easily fabricated in this way from a single strip, but I-shaped sections can be produced only by spot welding two such channels back to back, involving considerable additional cost (*Figure 1*). For this type of construction it was important, therefore, to investigate whether channels could be used efficiently as beams and, if so, what type of special bracing had to be used to ensure favourable performance with the least amount of such bracing. This problem was approached both analytically and experimentally as one phase of an extensive research project on light gauge steel structures sponsored at Cornell University by the American Iron and Steel Institute.

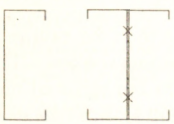

Figure 1

The performance of a channel loaded in the plane of the web can be visualized most simply by thinking of a single load P at midspan and considering the displacement of the

midspan section as proceeding in the successive stages depicted in *Figure 2*. The section, then, is thought of as being first displaced downward in simple translation. The stresses induced would be those of the ordinary beam theory and are indicated in character by the appropriate signs at the corners of the section.

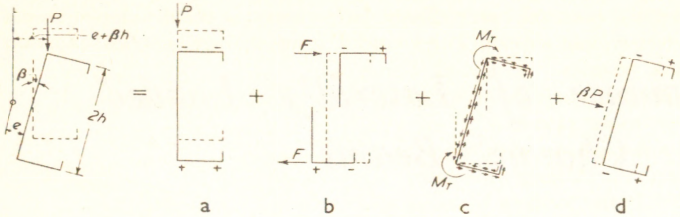

Figure 2. $F \times 2h + 2M_T = P(e + \beta h)$
— is compression, + is tension

Next, the channel is considered as cut and the two halves displaced much like two individual beams, resulting in the appropriate indicated corner stresses. To fit the two halves together they are next rotated about their individual shear centres, giving rise only to shear stresses of the ordinary St Venant character. In this inclined position, finally, the component of the vertical load parallel to the major axis causes additional bending about the minor axis, with its corresponding normal stresses. This picture is not an exact one but is discussed only to indicate the general type of the resulting stress distribution ; it will be found later that this simplified concept, somewhat modified, leads directly to an entirely satisfactory approximate analysis for design purposes. It is evident that under such a stress distribution cross sections distort out of their original plane ; for this reason the stresses associated, in particular, with the displacement stage b of *Figure 2* are generally known as warping stresses.

This simplified manner of visualizing the process cannot serve as a basis for a precise theory. In particular, the stresses arising from the various types of displacement cannot be computed rigorously by means of elementary theory from the various displacements of *Figure 2*. For this reason an accurate theory of the behaviour of transversely loaded channels must start from the basic equations of equilibrium of the problem.

THEORY

The general theory of torsional-flexural behaviour of thin walled members of open cross section has been discussed most recently by TIMOSHENKO[1] and GOODIER[2] ; most of their work, however, was oriented on the determination of critical buckling loads, whereas the present problem is one of stress determination under stable conditions. The general equations of equilibrium, adapted from the above sources to the particular problem of a channel under essentially vertical transverse load may be written as :

$$\begin{aligned} M_\xi &= -EI_x v'' = M_x + \beta M_y - u' M_z \\ M_\eta &= EI_y u'' = -\beta M_x + M_y - v' M_z \\ dM_\zeta/dz &= GC\beta'' - E\Gamma\beta'''' = u'' M_x + v'' M_y + m_z \end{aligned} \qquad \ldots\ldots(1)$$

The location of the fixed coordinate system x, y, z with the shear centre at the origin, is shown on *Figure 3* ; ξ, η, ζ are the corresponding displaced cross sectional axes. The resultant of the force system acting on the portion of the member to the right of any section may be represented by a force vector applied at the shear centre of the section,

plus a resultant moment. Then M_x, M_y, and M_z are the components of the latter parallel to the x, y, z axes and m_z is the intensity of the moment about the shear centre axis of a distributed load, if such is present. I_x and I_y are the principal moments of inertia of the cross section, C is the torsional constant (very closely $\frac{1}{3}st^3$, where s is the developed length of the centre line of the section and t its thickness) and Γ is another geometrical constant referring to the warping stresses. u, v and β are the displacements of the section indicated on *Figure 3* ; one, two or more primes (′, ″ *etc*) refer to the first, second *etc* derivatives with respect to z. E and G are, respectively, Young's modulus and the shear modulus. If the loading plane is parallel to one of the principal planes, such as for an unbraced channel loaded in the plane of its web, $M_x = M$ and $M_y = 0$. Neglecting certain terms which can be shown to be of higher order, the three equations 1 reduce to

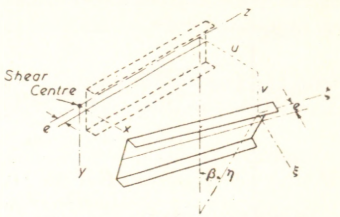

Figure 3. Note that z and ζ axes are a distance ' e ' behind the back of the channel

$$E\Gamma\beta'''' - GC\beta'' - \frac{M^2}{EI_y}\beta = -m_z \qquad \ldots\ldots(2)$$

This is the general equation for the problem considered in this paper.

For the specific case of the simply supported channel of length $2l$, and depth $2h$, which is subject to a single concentrated load $2P$ applied at midspan at the top of the web, $M = P(l - z)$, $m_z = 0$. An approximate solution may be obtained satisfying the following conditions :

$$\beta'(0) = \beta(l) = \beta''(l) = 0\ ; \quad \beta'''(0) = \frac{P[e + h\beta(0)]}{E\Gamma}$$

The origin of coordinates is located at midspan. The indicated value of $\beta'''(0)$ is obtained by integrating the left and middle expression of the third of equations 1 and noting that, at midspan, $\beta' = 0$ and $M_\zeta = -P[e + h\beta(0)]$ as can be seen from *Figure 2*.

The details of the derivation of equations 1 and the resulting solution are developed in a doctoral dissertation* by one of the co-authors and will be omitted here.

STRESSES IN UNBRACED CHANNELS

The practical results of this analysis, for one particular channel, are shown on *Figure 4* in a manner which facilitates evaluating their significance for design use. The usual criterion for design purposes (with respect to which reservations will be made later in this paper) would stipulate that the carrying capacity of the member is reached when yielding starts in the most highly stressed fibre. For a beam with no tendency to twist (*Figure 1*b) this means, as usual, that the maximum fibre stress $\sigma = Mh/I$ becomes equal to the yield point. In a channel, however, this fibre stress corresponds only to the first of the four displacements (a of *Figure 2*) and is augmented at the most highly stressed point (upper left corner) by the additional stresses from displacements b and d of that figure. To assess the reduced efficiency of a channel section (*Figure 1*a) as compared to a similar section prevented from twisting (*Figure 1*b) it is simplest to plot against the span length that simple bending stress $\bar{\sigma} = Mh/I$ which will result in yield stress at the most unfavourable fibre. For a section as *Figure 1*b, discounting the possibility of lateral

* Lansing, W. Stresses in Thin Walled Open Section Beams due to Combined Torsion and Flexure *Ph.D. Thesis* Cornell, 1949. of this dissertation is deposited with Professor Pugsley and available for reference.)

buckling, $\bar{\sigma}$ and the yield stress are equal. For the channel, *Figure 1*a, $\bar{\sigma}$ is smaller than the yield stress by the amount of the additional stresses induced by the asymmetry of the section. It is this information which has been plotted on *Figure 4*, for a yield point of 33,000 lb/in² (2,320 kg/cm²) for mild structural steel. On the same figure are shown the angles of rotation at midspan β (0) which obtain when yielding begins in the left upper corner.

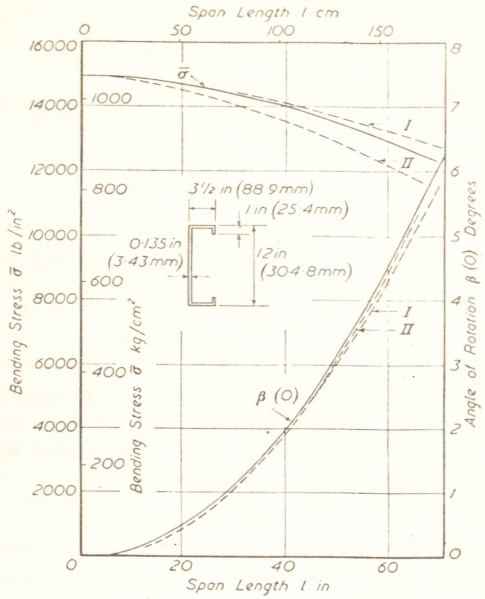

Figure 4. Analysis results for channel beam indicated

Several conclusions can be drawn from this diagram. It is seen that even for impracticably small spans, say up to 20 in (50·8 cm), the channel can carry only less than half the load which each channel of the symmetrical section of *Figure 1*b could carry before yielding is initiated. This is in sharp contrast to the performance of unbraced I- and Z-sections which, for very short spans, can be subjected to a moment such that $\bar{\sigma} = Mh/I$ = yield point and in which $\bar{\sigma}$ must be reduced only for larger spans because of buckling for I-beams and of twisting for Z-sections. (An analysis of the behaviour of Z-sections is also given in the previously quoted dissertation.) This difference caused by the off-centre location of the shear centre results in a primary twisting moment in channels: in I- and Z-sections, on the other hand, the shear centre and the centroid are coincident, so that torsional moments are merely caused by the rotation of cross sections and the deflection of the axis of shear centres out of a plane parallel to the loading plane. It is further seen that $\bar{\sigma}$ decreases relatively slowly with increasing span, indicating that no significant improvement of efficiency can be obtained by span reduction. Finally, for spans of reasonable magnitudes the central rotations are seen to become quite significant, practically.

ANALYSIS OF BRACED CHANNELS

If this analysis is to be extended to channels with intermediate braces it will be recognized that the resulting equations are likely to become too involved for practical design work. It is interesting, therefore, to study the influence of certain simplifications that can be made in the analysis for determining β. To begin with, the relatively small magnitude of the angles suggests that the influence of bending about the minor axis (*Figure 2*d) is likely to be small. Omission of the affected terms in the complete solution, yields an expression which plots as curve *I* in *Figure 4*. It shows, indeed, that such an approximation can be made safely. Next, in thin walled sections, the torsional constant C, being proportional to t^3, is always small as compared with other dimensionally identical cross

sectional properties which are proportional to t, such as I_x and I_y. This suggests that the resistance to twist caused by the shearing stresses, being proportional to C (*Figure 2c*), could possibly be neglected as compared with the resistance caused by the type of deformation indicated in *Figure 2b*. If this additional approximation is made, the curve *II* in *Figure 4* results, which is seen to be in error with respect to $\bar{\sigma}$ not exceeding about 7 per cent on the safe side. The error caused in magnitude of the rotation β is seen to be negligible.

This indicates that the torsional moment $P[e + \beta(0)h]$, *Figure 2*, is essentially resisted by the action depicted in *Figure 2b*. That is, each half of the section performs as if it were a simple beam, acted upon by the forces

$$F = \frac{P[e + \beta(0)h]}{2h} \qquad \ldots\ldots(3)$$

Since the location of loads F on this fictitious horizontal beam, and its span, are identical with those of the channel as a whole (for vertical bending), the resulting horizontal bending moments and the corresponding stresses shown in *Figure 2b* are directly proportional to those caused by vertical bending (*Figure 2a*), except for the minor influence of $\beta(0)$.

The action of intermediate bracing is now easily visualized. It prevents horizontal displacement of the fictitious half-beams at the points of bracing ; consequently, these half-beams are converted from simple beams of span length equal to that of the entire channel to continuous beams with individual spans equal to the distances between braces. If, for example, the braces were applied at the third-points of the span, the ' half-beam ' would perform as the continuous beam shown in *Figure 5* loaded by the force F as given by equation 3. The resulting maximum horizontal bending moment on the ' half-beam ' and the corresponding stresses of *Figure 2b* are less than one quarter of those obtained without bracing, as can be verified easily by continuous beam analysis.

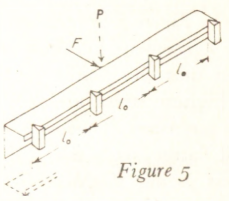

Figure 5

This reasoning is easily restated in a more general way. The indicated approximations are identical to equating to zero the second and third terms on the left of equation 2. The resulting equation

$$E\Gamma\beta'''' = -m_z \qquad \ldots\ldots(4)$$

is seen to be identical in form to that of a beam of rigidity $E\Gamma$ subject to loads of intensity m_z in which the deflection of the beam corresponds to β of the channel. Intermediate braces will therefore affect β and the corresponding stresses in the same manner as the deflections and stresses would be affected by intermediate supports in the corresponding continuous beam.

TESTS

To obtain experimental information on the behaviour of channels under various conditions of bracing, seven different types of thin walled channels were tested. Their depths ranged from 4 to 8 in (101·6 to 203·2 mm), the widths from 2·5 to 4 in (63·5 to 101·6 mm), and the thicknesses from 0·060 to 0·151 in (1·52 to 3·84 mm) while the lips were about $\frac{3}{4}$ in (19 mm) for all sections. These were tested under the following conditions : *1* spot welded back to back (*Figure 1b*) which is equivalent to continuous bracing, *2* braced as

in *Figure 6* with half-distance of bracing $l_2 = 33$ in (0·838 m), *3* braced as in *Figure 6* but with $l_2 = 45$ in (1·143 m) and *4* unbraced. Length of vertical span and location of loads was always as shown in *Figure 6*. Loads were applied through multiple ball bearings and knife edges to allow lateral and rotational motion as free from frictional restraint as was possible to achieve in a hydraulic testing machine.

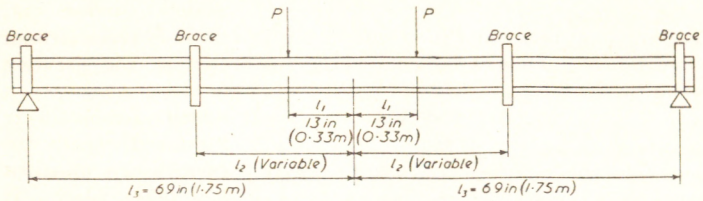

Figure 6. Experimental arrangement for testing beams

For the second condition theoretical stress determinations were carried out on the basis of the theory developed previously. The boundary and continuity conditions for equation 2 were adjusted to represent the situation of the test beams *i.e.* $\beta = 0$ at both ends and at the braces. In order to simplify calculations, advantage was taken of one of the simplifications discussed in connection with *Figure 4*, namely, the approximation of omitting the influence on β of bending about the minor axis (curve *I* on *Figure 4*) which was found to be negligible. (This amounts to neglecting the β term in the second of equations 1. Remembering that in these equations $M_y = 0$, this makes the third term on the left of equation 2 vanish.)

On *Figure 7* are shown the measured and computed stresses in that channel for which the agreement between experimental and theoretical values was least satisfactory. It is seen that the points of highest stress are the junctures of web and flange, with the stress being slightly larger at the upper one of these two points. These maximum stresses will govern practical design; the theoretical values are seen to agree with those from tests within about 11 per cent. In the other channels thus evaluated the discrepancy at stations *1* and *3* ranged from 2 to 11 per cent. Agreement is seen to be quite satisfactory also for station *4* in *Figure 7*, but is definitely unsatisfactory for station *2*.

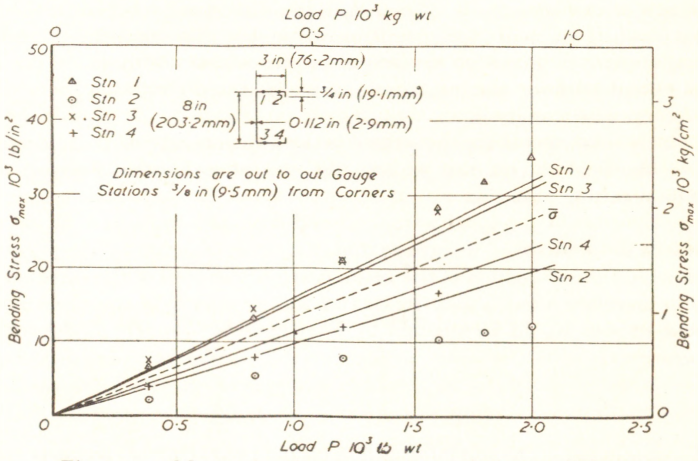

Figure 7. Measured and computed stresses in least satisfactory test channel

Measured midspan rotations considerably exceeded those obtained from the analysis.

This led to the suspicion that the bracing frames had not been rigid enough to prevent rotation at these points, as assumed in the theory. Subsequent tests showed this to be so. Indeed, rotations at the braces were found to amount to from 0.25 to 1° for the chosen loads, which represented about 10 to 30 per cent of those at midspan at the same loads.

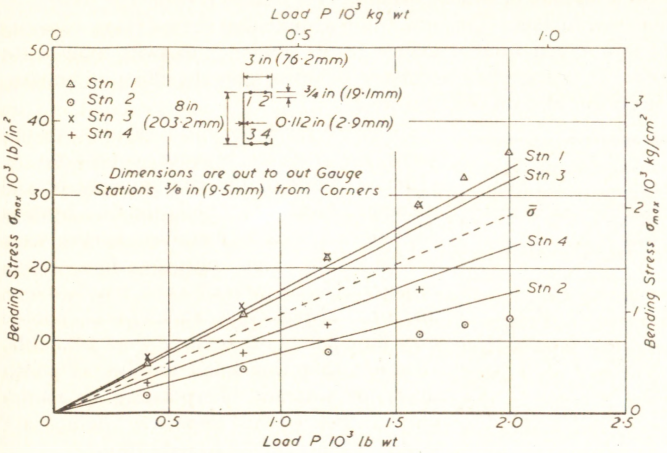

Figure 8. Comparison of measured stresses with corrected theoretical values

Since these tests were subsequently and separately carried out, there is no assurance that in the previous main tests, in which strains were measured, exactly the same brace rotations had taken place. It is possible to correct the theoretically computed stresses for these additional rotations, with reasonable accuracy. *Figure 8* allows a comparison of the measured stresses with the theoretical ones so corrected, for the same beam as in *Figure 7*. It is seen that the discrepancy between theory and test is reduced to less than half the previous value by this correction, and that theoretical and experimental maximum stresses now agree within about 5 to 6 per cent. This agreement is even better for the other tests in which the discrepancy between test and uncorrected theory was smaller than that shown on *Figure 7*. It should be noted that in flexural thin walled members the cross sections distort out of their original shape to a degree which depends on the width and thickness of the flanges and the depth of the member[3, 4]. This distortion, though small in practical terms, is likely to affect the distribution of the longitudinal stresses over the section, a factor which is not accounted for in the analysis.

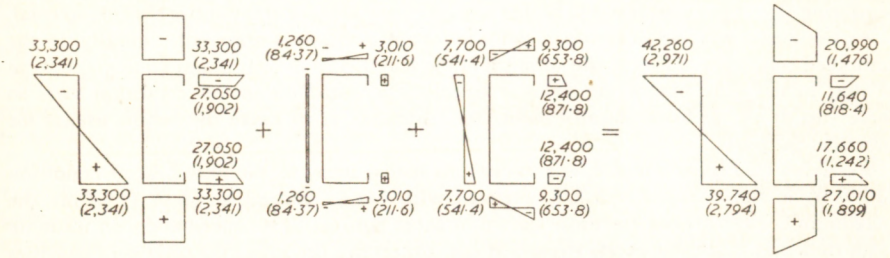

Figure 9. Stress distribution lb/in² over cross section. Figures in parentheses denote corresponding values in kg/cm²

Although the maximum stress is usually supposed to govern the strength of a member,

this is quite doubtful here. The stress distribution over the cross section, as is evident from *Figures 2* and *7*, is as shown in *Figure 9* (for the same channel as on *Figures 1* and *8*). The high corner stresses are seen to be quite localized. In a ductile material like mild steel, if the localized stresses reach the yield point, one would merely expect a redistribution to take place so that the hitherto understressed portions of the flanges provide the additional resistance if loads are increased further. One must then assume that the carrying capacity of a channel is affected to a much smaller degree by its tendency to twist than is the localized maximum stress. It is therefore necessary to investigate the effect of bracing, not only on maximum stress but also on ultimate load.

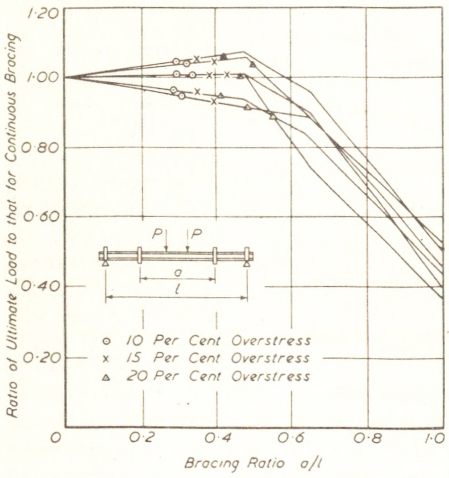

Figure 10. Effect of use of bracing. Curves have been corrected for yield points of steels

Figure 10 gives the ratios of ultimate test loads for various bracing conditions to ultimate loads of the continuously braced member (*Figure 1b*). Only the four bracing conditions *1* to *4* as described earlier were available for this purpose, for which, respectively, the ratio a/l was 0, 0·478, 0·652, and 1·0. Therefore, for each type of channel only four points on its curve were available. It is felt that this small number of points does not warrant interpolating a smooth curve ; hence the respective points are merely connected by straight lines.

It is seen that for the smaller of the two spacings of braces ($a/l = 0{\cdot}478$) ultimate loads for all practical purposes are the same as for continuous bracing. Ultimate test loads are here defined as those at which the beam continues to deflect under constant load. This point is somewhat indefinite and depends on speed of loading and also on the details of the stress/strain curve even for steels of identical yield point. These tests were carried out by several different investigators, which introduces a personal equation into such determinations. Some differences were found also in the stress/strain curves of the steels of which dimensionally identical channels were formed. For these reasons the scattering of ± 7 per cent seems to be due to experimental inaccuracy and is entirely normal.

At the larger spacing of braces a definite loss of strength is apparent. Finally, in the unbraced condition ($a/l = 1$) the strength of the members was only about 40 to 50 per cent of that in the fully braced condition. In addition, rotations in this condition were so large (up to 15° at loads slightly below the ultimate) as to make the beams useless for practical purposes.

Referring to *Figures 7* and *8*, the maximum flange stress in the fully braced condition ($a/l = 0$) is the usual $\bar{\sigma} = Mh/I$, whereas with braces spaced at 66 in (1·68 m) the maximum corner stresses are those shown in those figures. The information on ultimate loads indicates that these excess stresses at the corners did not affect the carrying capacities to any practically significant degree for this location of braces. For braces spaced farther apart the difference between $\bar{\sigma}$ and the maximum corner stress increases further and results in a gradual lowering of the carrying capacity.

ALTERNATIVE DESIGN REQUIREMENTS

For design purposes it is now possible to take one of two positions. Conservatively, one can stipulate that the maximum corner stress shall not exceed the yield point for a load equal to the design load times the factor of safety. Here the use of a single channel with discrete bracing will always be less economical than one with continuous bracing (*Figure 1*b) since the corner stress in the former always exceeds that of the latter for the same load. This difference decreases with decreasing spacing of braces. Alternatively, one can take advantage of the reserve strength by plastic stress redistribution, as illustrated by *Figure 10*. Then one could stipulate that channels may be designed such that the uncorrected $\bar{\sigma} = Mh/I$ shall be equal to the yield point at the design load times the safety factor, provided braces are so spaced that the difference between the maximum corner stress and $\bar{\sigma}$ shall not exceed a specified fraction of $\bar{\sigma}$. This fraction must be so specified that it shall not adversely affect the carrying capacity *i.e.* such that its effect would be obliterated by plastic redistribution. On the basis of the experimental evidence the authors lean toward the latter more liberal approach.

To determine what fraction should be specified for this purpose, additional information is shown on *Figure 10*. On each curve, in that figure, three points are shown designated respectively as 10, 15 and 20 per cent overstress. They indicate the values of a/l for which the difference between the maximum corner stress and $\bar{\sigma}$, as determined by theory, amounts to the respective percentages of $\bar{\sigma}$. It is seen that a 15 per cent overstress does not affect the carrying capacity significantly, whereas the 20 per cent points are usually definitely located on or near the parts of the curves which show a marked downward trend. It would seem, therefore, that within the limits of our test evidence, a theoretical overstress of about 15 per cent can be disregarded in practical design. The problem is then, merely, to locate braces such that no more than this overstress will occur.

SIMPLIFIED STRESS DETERMINATION

For either of these alternative design methods it is necessary to compute the overstress for a given arrangement of loads and braces or *vice versa* to determine required location of braces for given loadings and a stipulated overstress. It is evident that the detailed theory briefly discussed before is much too elaborate to serve this purpose in routine design practice. However, various approximations can be made in the general theory, as has been discussed in detail in connection with *Figure 4*. These make it possible to devise a very simple method which allows the determination of maximum corner stresses with very good accuracy.

It was shown there that consideration of displacements a and b of *Figure 2*, without regard to c and d, gives results very close to the values of the accurate theory. If the half-beams of *Figure 2*b were regarded as simple beams acting in a manner as shown on *Figure 5*, the individual stress distributions from simple beam theory for displacements a and b would be as shown by *Figure 11* a and b. This distribution is obviously impossible since, according to *Figure 11*b, a stress discontinuity would occur in the web at mid-height, so that the superposition of the distributions of *Figures 11*a and b would not result in that of *Figure 9*. Hence, the distribution in the horizontally bending half-beams must be approximated by one of the general nature of *Figure 11*c. This can be done by using, instead of the full half-depth of the web, an equivalent partial depth for computing cross

sectional properties of the half-beam. This concept of effective length, width or area is frequently used in many other instances, particularly in the field of thin walled members[3, 4]. Here it merely requires the replacement of the non-uniform stress distribution in the web by an equivalent uniform distribution such that the governing maximum stresses remain

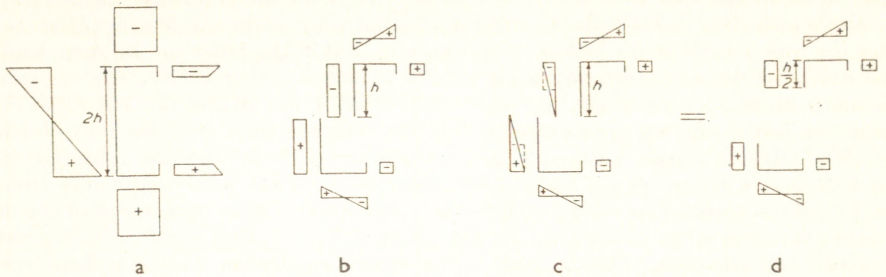

Figure 11. Individual stress distributions from simple beam theory

unaffected. In other words, the actual triangular distribution in the web, *Figure 11*c, is replaced by the dotted rectangular one of equal maximum intensity and equal total area. Then corner stresses can obviously be computed from the cross sectional properties of the section shown on *Figure 11*d where only one quarter of the web is regarded as effective for each half-beam. For channels without stiffening lips it can be shown on theoretical grounds that a somewhat closer approximation is obtained if one sixth of the web is regarded as effective for either half-beam.

The manner of determining the corner stresses with very good approximation is, therefore, the following : stresses caused by vertical bending (*Figures 2*a, *11*a) are determined as usual. For horizontal bending (*Figures 2*b, *11*d) the cross section of each half-beam is regarded as consisting of the flange, lip and one quarter of the web. This beam is loaded horizontally at all points where vertical loads P act on the channel by the corresponding horizontal loads $F = P\,e/2h$ (equation 3 with $\beta(0)h$ neglected as small in comparison with e). For distributed vertical load p the corresponding distributed horizontal load, of course, is $f = pe/2h$. Each half-beam, so loaded, represents a continuous beam supported at the braces, as shown for one particular case on *Figure 5*. Stresses from this horizontal bending are computed in the usual manner and superposed on those from vertical bending to result in the maximum corner stresses.

For the four dimensionally most extreme of the seven test channels, comparative values have been computed from this approximate approach and from the theory proper, for two different load values each. The discrepancies between the two methods of computation are shown in *Table I*. It is seen that the critical maximum stresses in the corners (stations *1* and *3*) are obtained with ample accuracy by this simplified approach. Discrepancies are larger for stations 2 and 4. These, however, are generally not critical since stresses there are usually smaller than at *1* and *3*. Stresses at all four points by the approximate method are obtained smaller than computed from the more accurate theory.

Table I

Station	Deviation per cent	
	Mean	*Maximum*
1	− 2·5	− 5·2
2	− 3·2	− 12·9
3	− 1·1	− 5·2
4	− 8·8	− 16·1

Figure 12

The 10, 15 and 20 per cent points on *Figure 10*

were computed by this approximate method, since it is this approach which is likely to be used in routine design for determining the required spacing of braces.

BRACING DISTANCES, ROTATIONS, LATERAL FORCES

If the overstress criterion is adopted for design purposes, the safe distances between braces are determined from the requirement that the corner stress in the continuous half-beam (*Figures 5* and *11c*) shall not exceed $\bar{\sigma}$ by more than the stipulated percentage. This merely requires ordinary continuous beam analysis. Analyses carried out in the aforementioned thesis (* p 51) for a great variety of practical loading schemes show that it is never necessary to provide more than four braces between supports in order to limit the overstress to 10 per cent of $\bar{\sigma}$. If 15 per cent overstress is accepted for practical design, as was previously suggested on the basis of *Figure 10*, similar calculations show that three braces equally spaced between supports will satisfy this requirement for most practical loadings. A single concentrated load at or near midspan represents an unfavourable exception ; this is most easily dealt with by locating a brace directly at the load point.

As a last point, the order of magnitude of rotations at midspan under design loads may be of interest in channels so braced. For this purpose *Figure 13* has been prepared. It shows the rotations as actually measured in tests, for a load resulting in central vertical deflections equal to span/360. In the United States this is often considered to be the maximum allowable deflection under load *in situ*, particularly when plastered ceilings are suspended from the floor. The overstress criteria of 10, 15 and 20 per cent are shown as on *Figure 10*. If the 15 per cent criterion were adopted, rotation under load would not exceed about 1·5°. These measured angles include the additional rotations at midspan caused by rotation at the braces, the bracing frames not being rigid enough to restrain the channel completely. This situation may well occur in practical installations.

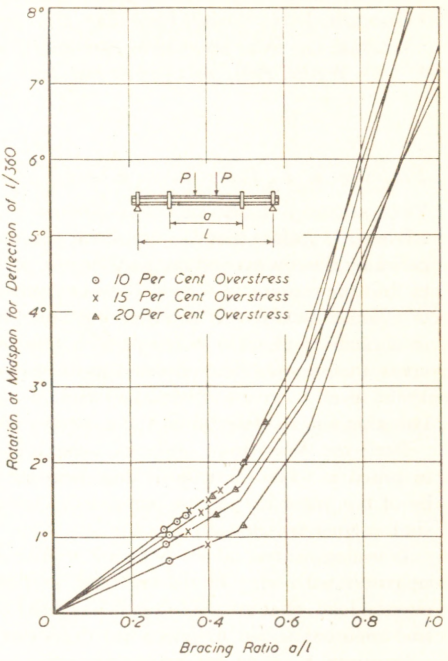

Figure 13. Rotations for a load resulting in central vertical deflections equal to span/360

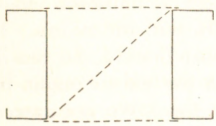

Figure 14

Braces may be applied in the manner shown on *Figure 14*. If channels are placed in pairs with webs facing each other, attachment to rigid floor and ceiling systems without diagonals may, under favourable conditions, serve as satisfactory bracing. The force that the brace has to withstand is easily determined by the approximate method of calculation.

Indeed, as is evident from *Figure 5*, the horizontal forces in the braces are simply the horizontal reactions of the half-beam.

Department of Structural Engineering
Cornell University, Ithaca
New York, U.S.A.

(*Received June 1949*)

REFERENCES

[1] TIMOSHENKO, S. *J. Franklin Inst.* 239 (1945) 201, 249, 343
[2] GOODIER, J. N. *Cornell Univ. Eng. Exp. Stn Bulls* Nos. 27, 1941 and 28, 1942
[3] WINTER, G. *Nat. adv. Comm. Aeronautics, techn. Note* No. 784, 1940
[4] — *Prelim. Publ. 3rd Congress Int. Assoc. Bridge Struct. Eng.* (1948) 137

Discussion

Professor J. F. Baker in the Chair

PROFESSOR J. F. BAKER was pleased to hear a simple yet rational design method advocated, rather than an empirical approach to the design problems. Describing experimental work carried out at Glasgow, R. KENEDI said that an attempt had been made to find the spacing of lateral bracing equivalent to continuous support. Lateral bracing of channel beams was achieved by attaching tension wires to either side of the beam at a pitch of about 6 in (*c* 15 cm). The central lateral deflection was taken as a convenient criterion. The required ratio of beam length to brace spacing was found to be about seven to give support approximately equivalent to continuous bracing ; the corresponding ratio suggested in the present paper appeared to be two.

Professor WINTER, in reply, said that the use of seven braces was quite uneconomical in practice. The increase in deflection arising when only two braces were used would be of the order of 5 to 10 per cent. This corresponded to the usual tolerance in most civil engineering designs.

It was suggested by W. MERCHANT that the results of WINTER and KENEDI could not be correlated owing to the variation in rigidity of the two types of bracing used. He observed also that no experiments had been carried out on beams in which the two flanges had been connected to give some degree of bracing.

Professor N. J. HOFF stated that an American company had solved the problem of avoiding twisting by applying the loads at the shear centres with the aid of brackets. He would be interested to learn how the problem of solving the fourth order differential equations with variable coefficients had been overcome. Professor WINTER replied that, after assuming different forms for β, it was found that large differences in β had little effect on the result. Assuming a convenient form for β, an approximate solution could be found.

H. L. Cox asked whether the first order effects of distortion of the cross section of the beam had been considered. The effect was dependent primarily upon the width to thickness ratios employed. Professor WINTER considered that the width to thickness ratios were such as to eliminate the possibility of local buckling occurring in the beams. It was pointed out by H. L. Cox that when the load is applied to the web of a channel beam, distortion of the cross section would almost certainly occur and the effects might be larger than the secondary effects of the distortion considered. Professor WINTER agreed that these effects might be important ; however, they had received no theoretical treatment in this work.

Performance of Compression Plates as Parts of Structural Members

G. WINTER

A number of recent investigations are reviewed on the behaviour of compression plates as parts of structural members, in contrast to that of isolated plates. This paper does not present any new results but, by request, was intended as a review of this particular topic. For this reason the text that follows merely represents a brief abstract of the talk delivered at the symposium. An extensive bibliography is appended.

THE small deflection theory of buckling of flat compression plates is governed by the equation

$$\frac{\partial^4 w}{\partial x^4} + 2\,\frac{\partial^4 w}{\partial x^2 \partial y^2} + \frac{\partial^4 w}{\partial y^4} + \frac{\sigma_x t}{D}\,\frac{\partial^2 w}{\partial x^2} = 0 \qquad \ldots\ldots(1)$$

Solutions for individual plates with various edge conditions (free, simply supported, fixed) were first obtained by BRYAN and, for a great variety of load and edge conditions, by TIMOSHENKO.

In actual structures such plates with ideal end conditions occur rarely, if ever. In a box shaped column, for example, the four plates forming the box support each other mutually so that each of them is elastically supported along its longitudinal edges. The problem of the performance of such interacting plates, just as for disjointed plates, must be discussed in two separate phases : *a* the critical or buckling condition, *b* the post-buckling behaviour.

The first approximate method for determining buckling stresses of plate assemblies was given by BLEICH in 1924. The problem consists of the solution of equation 1, the boundary conditions of which must be adjusted according to the physical problem at hand. For a box shaped column, *Figure 1*, the plates with the larger width/thickness ratio can be regarded as the ' buckling plates ', and the others as the ' restraining plates '. Conditions of continuity require that along the common edges, for stiff joints,

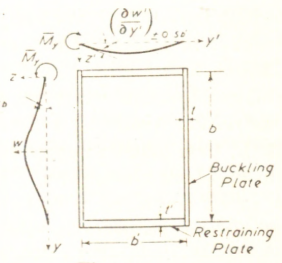

Figure 1

$$\frac{\partial w}{\partial y} = \frac{\partial w'}{\partial y}$$

This condition requires that the length of buckling waves is the same in all four plates, and hence can be determined only by accounting rigorously for the interaction of all individual components. Bleich's solution is approximate chiefly in that it assumes the wavelength of the restraining plates to be equal to the width of

the buckling plates, and that the influence of longitudinal compression on the deformations of the restraining plates is accounted for by a simple magnification factor, rather than by rigorous theory.

BIJLAARD, in 1940, developed the exact theory of such interaction by setting up individual equations of the type of equation 1 for each of the individual plates, and solving this set of simultaneous equations with due consideration for continuity of stress and strain at the common edges. In 1943, LUNDQUIST, STOWELL and SCHUETTE developed a relaxation method for determining critical stresses of plate assemblies by a modified moment distribution procedure in a way similar to that previously given by Lundquist for investigating the stability of rigid-joint structural frames.

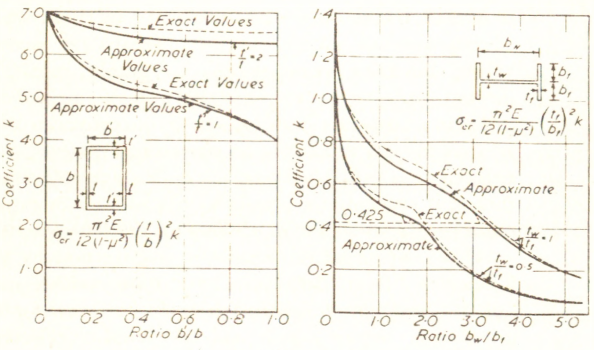

Figure 2

Figure 2 shows the results of such investigations as obtained by the latter two exact methods and by Bleich's approximate method for box shapes and for I-sections. The simpler Bleich method is seen to be sufficiently accurate for many engineering purposes. This figure is reproduced, by permission of Bleich, from a manuscript as yet unpublished.

Equation 1 holds only in the range of linear elasticity whereas in practical structures many if not most problems of this type arise in the stress range above the limit of proportionality. Here the basic equation must be modified as follows

$$A\frac{\partial^4 w}{\partial x^4} + 2B\frac{\partial^4 w}{\partial x^2\,\partial y^2} + C\frac{\partial^4 w}{\partial y^4} + \frac{\sigma_x t}{D}\frac{\partial^2 w}{\partial x^2} = 0 \qquad \ldots\ldots(2)$$

where A, B and C are functions, in general, of the secant modulus, the tangent modulus and Poisson's ratio. Indeed, in the above equation the first term is associated with longitudinal curvature in which direction the mean stress is above the proportional limit, the third term with transverse curvature in which direction the mean stress is zero and hence below the proportional limit, whereas the second term is mixed in nature and hence affected by both mean stresses. The problem, then, becomes anisotropic and different elasto-plastic constants apply to different terms.

A rather intuitive solution of this problem was given by BLEICH in 1924, resulting in quite satisfactory accuracy. Of the many later investigations of plastic plate buckling those in best agreement with test results were developed by BIJLAARD in 1940 and by STOWELL in 1948. Both are based on theories of plasticity of the deformation type and differ chiefly by the fact that Stowell, by way of simplification, assumes Poisson's ratio to be constant and equal to 0·5. The enumerated methods can and have been applied to the determination of critical buckling stresses of a great variety of structural members composed of flat compression plates.

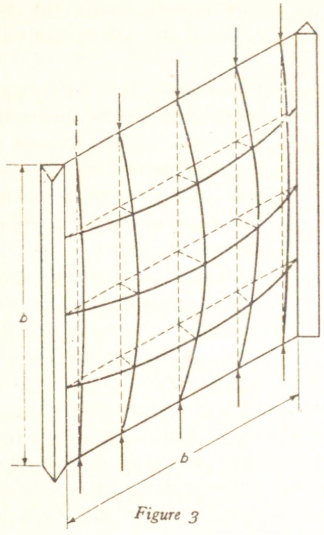

Figure 3

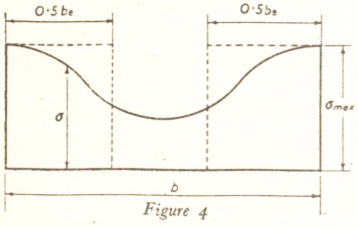

Figure 4

In contrast to columns which actually fail at or slightly below the theoretical critical load, compression plates, particularly if supported along both longitudinal edges, continue to carry increasing loads beyond those which theoretically cause initial buckling. The mechanism of this post-buckling action can be visualized from *Figure 3* in which a compression plate is replaced by an oversimplified bar lattice model. It is seen that post-buckling deflections, in contrast to column deflections, are restricted in magnitude by the restraining action of the horizontal bars and the tension stresses arising in them which correspond, in plates, to the membrane stresses. When buckling commences, it merely results in limited deflection and redistribution of the hitherto uniform compression stress which concentrates more and more near the edges, as shown in *Figure 4*. This behaviour is so marked, and the deflections so gradual, that it is difficult to establish critical stresses experimentally from strain or deflection measurements.

This post-buckling behaviour is governed by VON KÁRMÁN's ' large deflection ' equation, which justifies its designation inasmuch as it accounts for the membrane stresses but is still restricted to relatively small deflections to the extent that higher order terms are, as usual, neglected in the curvature expression. The equation reads

$$\frac{\partial^4 w}{\partial x^4} + 2\,\frac{\partial^4 w}{\partial x^2\,\partial y^2} + \frac{\partial^4 w}{\partial y^4} = \frac{t}{D}\left(\frac{\partial^2 F}{\partial x^2}\,\frac{\partial^2 w}{\partial y^2} - 2\,\frac{\partial^2 F}{\partial x\,\partial y}\,\frac{\partial^2 w}{\partial x\,\partial y} + \frac{\partial^2 F}{\partial y^2}\,\frac{\partial^2 w}{\partial x^2}\right) \quad . . (3)$$

where F is an Airy stress function.

A number of solutions of this problem, with various degrees of approximation, were developed by MARGUERRE, TIMOSHENKO, TREFFTZ, COX, LEVY and others. Most of them are rather involved mathematically and have been carried out numerically only for a few selected cases. They can generally be expressed in terms of the parameter σ_{cr}/σ_{max} where σ_{cr} is the critical stress obtained from the small deflection theory, equation 1, and σ_{max} is the edge stress as shown on *Figure 4*. The results are usually given in terms of an ' equivalent width ' of the buckled plate, a concept introduced by VON KÁRMÁN in 1932 and illustrated on *Figure 4*. That is, the equivalent width b_e is the combined width of the two broken line rectangles of that figure, the enclosed area of which is equal to the area under the actual curve of non-uniform stress distribution.

The most rigorous of these solutions is that by LEVY, which deviates but little from that of MARGUERRE and is rather well confirmed experimentally. Experimental results, however, depend largely on the degree of initial flatness of the plate and of centering of load, a fact which has been confirmed theoretically by HU, LUNDQUIST and BATDORF in

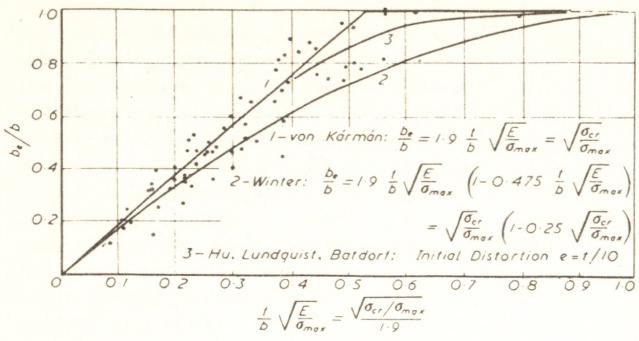

Figure 5

their investigation of the effect of small deviations from flatness on effective width. For this reason the author and others find it desirable to rely primarily on test results for the purpose of developing formulae for practical design use. His experimental results are shown on *Figure 5* together with the conservative expression (lowest curve) he proposed for design and which is incorporated in the *Specification for the Design of Light Gage Steel Structural Members*, Amer. Iron and Steel Institute. The curve designated by 3 gives the values obtained by Hu, Lundquist and Batdorf when the initial deviation from flatness is equal to one tenth of the plate thickness and, in shape, is equal to the natural buckling mode. It is indicated on the figure merely to show the order of magnitude of the effect of such small distortion, which confirms the supposition that the scattering usually obtained in such tests is caused chiefly by initial deviations.

The performance of a compression plate in the post-buckling range as it affects the behaviour of a beam of which it forms the compression flange is shown on *Figure 6*. As the load increases, the initially constant compression stress becomes more and more non-uniformly distributed, with a corresponding decrease of effective width and a continuous downward shift of the neutral axis. Results of two tests indicating the measured shifting of position of the neutral axis with increasing load are shown on the lower part of that figure. It is necessary, for such members, to compute effective cross sectional properties (area, moment of inertia, section modulus *etc*) which depend on the magnitude of σ_{max}. In such members, formed of mild steel, incipient failure occurs at loads equal to or slightly higher than those at which the edge stress σ_{max} reaches the yield point.

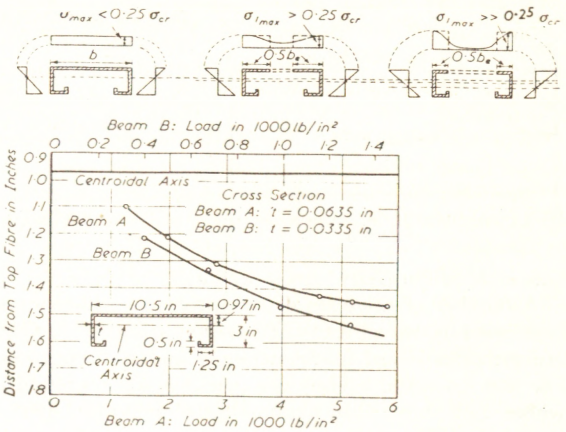

Figure 6

(*1 in = 2·54 cm; 1 lb/in² = 0·0703 kg/cm²*)

For thin walled compression members, such as box columns of which the components are stressed into the post-buckling range, it is necessary to modify the column curve for

locally stable sections of the same material *e.g.* curve $Q = 1{\cdot}0$ on *Figure 7*, to account for stress re-distribution in the component plates. This can be achieved in a rather approximate way by the introduction of a form or shape factor Q which is defined as the ratio of the ultimate strength of the thin walled short column ($L/r = 0$ in the limit) to the ultimate strength of the same short thin walled section if local buckling were prevented by suitable means.

Department of Structural Engineering
Cornell University, Ithaca
New York, U.S.A.

(*Received October 1949*)

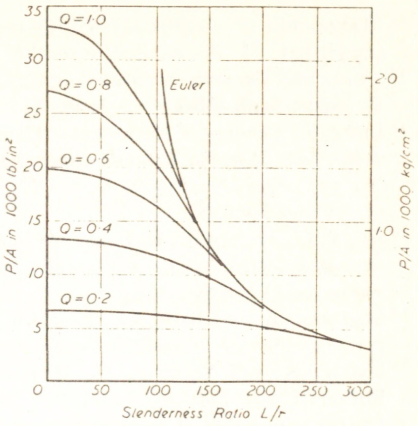

Figure 7

BIBLIOGRAPHY

Buckling stresses

[1] BRYAN, G. H., *Proc. London math. Soc.* 22 (1891) 54

[2] TIMOSHENKO, S. *Theory of Elastic Stability* New York, 1936

[3] BLEICH, F. *Theorie und Berechnung der Eisernen Brücken* Berlin, 1924

[4] BIJLAARD, P. P. Theory of the Plastic Stability of Thin Plates *Publ. int. Assoc. Bridge Struct. Engng* 6 (1940/41) 45

[5] — Some Contributions to the Theory of Elastic and Plastic Stability *ibid* 8 (1947) 17

[6] KOLLBRUNNER, C. F. Das Ausbeulen des Freistehenden Winkels. Das Ausbeulen der auf Druck beanspruchten Platten im elastischen und plastischen Bereich *Mitt. Inst. für Baustatik, Eidg. Techn. Hochschule, Zürich* Nos. 4, 1936 and 17, 1946

[7] LUNDQUIST, E. E. Local Stability of Symmetrical Rectangular Tubes *Nat. adv. Comm. Aeronautics tech. Note* No. 743, 1939
— Channel and Z-Sections *ibid* No. 722, 1939

[8] LUNDQUIST, E. E. and STOWELL, E. Z. Critical Compressive Stress for Flat Rectangular Plates Elastically Restrained *Nat. adv. Comm. Aeronautics Report* Nos. 733, 1942 and 734, 1942

[9] — — and SCHUETTE, E. H. Principles of Moment Distribution Applied to Stability of Structures Composed of Bars and Plates *Nat. adv. Comm. Aeronautics Wartime Report L-326*, 1947

[10] STOWELL, E. Z. A Unified Theory of Plastic Buckling *Nat. adv. Comm. Aeronautics tech. Note* No. 1556, 1948

Post-buckling behaviour, theory and tests

[11] VON KÁRMÁN, T., SECHLER, E. E. and DONELL, L. H. Strength of Thin Plates in Compression *Trans. Amer. Soc. mech. Engrs* APM 54–5, 54 (1932) 53

[12] COX, H. L. Buckling of Thin Plates in Compression *Aeronautical Res. Council Report and Memo.* No. 1554 London, 1933

[13] MARGUERRE, K. Effective Width of the Compressed Plate *Luftfahrtforschung* 14 (1937) 121

[14] — and TREFFTZ, E. Carrying Capacity of a Long Plate Beyond the Critical Stress *Z. angew. Math. Mech.* 17 (1937) 85

[15] LEVY, S. Bending of Rectangular Plates with Large Deflections, *Nat. adv. Comm. Aeronautics techn. Note* No. 846 and *Report* No. 737, 1942 ; also *techn. Note* No. 847 and *Report* No. 737 ; *Report* No. 740 ; *techn. Note* No. 853 (LEVY and GREENMAN) ; *techn. Note* No. 884 (LEVY and KRUPEN)

[16] HU, P. C., LUNDQUIST, E. E. and BATDORF, S. B. Effect of Small Deviations from Flatness on Effective Width and Buckling of Plates in Compression *Nat. adv. Comm. Aeronautics techn. Note* No. 1124, 1946

[17] SCHUMAN, L. and BACK, G. Strength of Rectangular Flat Plates Under Edge Compression *Nat. adv. Comm. Aeronautics Report* No. 356, 1930

[18] LAHDE, R. and WAGNER, H. Experimental Determination of Effective Width of Buckled Plates, *Luftfahrtforschung* 13 (1936) 214

[19] FRANKLAND, J. M. The Strength of Ship Plating Under Edge Compression, *U.S. exp. Model Basin Rep.* No. 469, 1940

[20] HEIMERL, G. J. Determination of Plate Compressive Strength *Nat. adv. Comm. Aeronautics tech. Note* No. 1480, 1947

[21] WINTER, G. Strength of Thin Compression Flanges *Trans. Amer. Soc. civil Engrs* 112 (1947) 527 ; also *Cornell Eng. exp. Station Reprint* No. 32

[22] — Performance of Thin Steel Compression Flanges *Prelim. Publ. 3rd Congress Int. Assoc. Bridge Struct. Eng.* (1948) 137

Discussion

Professor A. J. S. Pippard in the Chair

R. KENEDI pointed out that tests at the Royal Technical College, Glasgow, had shown that plain thin walled channel sections did not carry increasing load in the post-buckling stage, as did the lipped channel sections discussed by the lecturer. He also suggested that the overall stability of the column affects the degree of edge fixity of the plate. Professor WINTER replied that there was in fact a small increase in post-buckling stress for a plain channel, although it was far smaller than with the lipped channel owing to the latter's greater degree of edge fixity. He pointed out that, in design, stresses higher than the critical stress were not used, for the sake of good appearance.

J. C. CHAPMAN drew attention to the very high extreme fibre stresses which occurred due to plate bending. The author agreed that these stresses would sometimes exceed the yield stress and that the procedure which he described must not be used for design in fatigue conditions.

Professor A. ROGGEVEEN described tests that he had made on the buckling of the webs of large welded boxes where the critical stress was reduced by an amount equal to the residual stresses left by the welding. Professor WINTER pointed out that his tests were carried out on small cold-rolled sections but agreed that residual stresses would affect the critical stress. W. S. HEMP doubted the soundness of the equivalent width assumption for use after buckling, and thought that a tangent modulus method should be used.

In a written contribution R. KENEDI drew attention to further results obtained at Glasgow, a number of which have already been published [KENEDI, R. M. and MOIR, C. M. *Structural Engineer* 26 (1948) 119]. He had found that the lower scatter boundary of the experimental results on their struts could be defined by a Perry-Robertson type of formula

$$p_c = \frac{p_y + (1 + \eta)p_e}{2} - \left[\left(\frac{p_y + (1 + \eta)\, p_e}{2} \right)^2 - p_y p_e \right]^{\frac{1}{2}}$$

taking

$$p_e = \frac{E}{1 - \sigma^2} \left(\frac{t}{b} \right)^2 \left[\frac{b/t}{46 + 0{\cdot}15 b/t} \right]$$

and

$$= 0{\cdot}0025 b/t$$

This formula gave results which agreed with those obtained from Professor WINTER's formula for the struts concerned.